

10 Earthquakes in Chile

SERGIO E. BARRIENTOS

No recorded human generation in Chile has escaped the damaging consequences of large earthquakes. More than ten events with magnitudes equal to or greater than magnitude 8 have taken place during the twentieth century alone. Among these earthquakes is the 1960 event, the largest earthquake ever recorded since the beginning of instrumental seismology. Such extreme seismic activity is a result of the interaction of the Nazca, Antarctic, Scotia and South American plates in southwestern South America where Chile is located (Fig. 10.1).

In general, seismogenic zones in Chile are basically well established: large shallow (0–50 km) thrust earthquakes along the coast; large deeper (70–100 km) tensional as well as compressional events within the subducting Nazca Plate; and very shallow seismicity (0–20 km) in a few places, such as the cordillera region of central Chile and the southern extremity of the continent by the Magellan Strait. Deeper seismicity (150 to 650 km) occurs further to the east, beneath Bolivia and northwestern Argentina (Figs 10.2 & 10.3).

The large thrust earthquakes, responsible for most of the damage recorded in history, are located along the coast from Arica (18°S, the northernmost extreme of coastal Chile) to the triple-junction at Taitao Peninsula (46°S). With magnitudes that can reach values well over eight, these events are usually accompanied by noticeable coastal elevation changes and, depending on the amount of seafloor vertical displacement, by catastrophic tsunamis. Their rupture zones are limited to the coupled region between the Nazca and South American plates which extends down to 45–53 km depth (Tichelaar & Ruff 1991) and their lengths could reach well over 1000 km. Their spatial and time characteristics have been studied (Kelleher 1972; Barrientos 1981; Martin 1991; Nishenko 1985; Ramírez 1988; Beck *et al.* 1998), so that the hazard due to these large events is well recognized and understood. Return periods for magnitude 8 events are of the order of 80 to 130 years for any given region in Chile, but about 12 years when the country is considered as a whole. Megathrust earthquakes seem to have much longer return periods, of the order of a few centuries for any given region (Cifuentes 1989; Barrientos & Ward 1990; Cisternas *et al.* 2005). The 1939 Chillán event does not belong to this suite of thrust earthquakes; however, it has been the most damaging earthquake in terms of loss of human life in Chilean history.

North of the Chile triple-junction, the Nazca Plate is being subducted beneath South America (SA) at a rate of about 65 mm/year (Angermann *et al.* 1999). South of the junction as far as 57°S, the Antarctic Plate (AN) is being subducted at a considerably slower rate, between 10 and 20 mm/year (Pelayo & Wiens 1989). The slow convergence rate and the type of subducted structures are probably the main reasons for the relative lack of seismicity on the western margin of South America south of the Chile triple-junction. The fundamental tectonic difference between the region north of the triple-junction and that to the south is that the Chile Ridge has been recently subducted in the latter.

South of the western end of the Magellan Strait (*c.* 52°S), the AN is no longer being subducted under the SA, but under the Scotia Plate (SC) (Winslow 1982; Pelayo & Wiens 1989; Klepeis

1994), so that the southernmost tip of South America is not on the SA but on the SC. The SA–SC boundary is a diffuse boundary displaying mostly left-lateral strike-slip relative motion, which runs approximately along the Magellan Fault (Katz 1964), from the easternmost tip of Tierra del Fuego (Strait of Le Maire) along Lake Fagnano, Seno Almirantazgo and into the NW Magellan Strait. North of *c.* 52°S, the SA and AN converge normally at a rate of 19 mm/year. South of this point, part (*c.* 7 mm/year) of the convergence rate is accommodated by the SA–SC boundary along the Magellan Fault, and the AN and SC converge at a lower rate of 13 mm/year. Historical earthquakes in 1879 and 1949 (in which two events took place on 17 December, separated by about 8 hours), all of them with estimated magnitudes above 7, are the largest earthquakes recorded in the region.

More recently, the hazard produced by large, intermediate-depth tensional earthquakes within the subducting Nazca Plate has been recognized. These events are caused by faulting within the subducting plate at depths between 80 and 110 km with apparently high stress drops (Kausel 1991). Extreme examples of these type of events are the *M* = 8 Calama earthquake in 1950 (Kausel & Campos 1992), the *M* > 8 Chillán event in 1939 (Beck *et al.* 1998) and the most recent large event (*M* = 8.0) of 30 June 2005 which took place within the Nazca Plate about 200 km east of Iquique, the largest city in the region. Malgrange & Madariaga (1983) have reported a suite of tensional events of this type within the Nazca Plate in the > 7 magnitude range, of which the 1965 La Ligua event stands out for the destruction it produced.

Additionally, complex stress interaction gives rise to down-dip compressional events at about 60–70 km depth. These events can reach magnitudes over 7, as recently reported by Lemoine *et al.* (2001) and Pardo *et al.* (2002b), in particular for the very damaging earthquake of October 1997 near Illapel.

Another seismogenic region, which has become the subject of recent studies, is that located at shallow depths in the Andean cordillera in the central part of Chile. Godoy *et al.* (1999) and Barrientos *et al.* (2004b) have carried out structural and seismicity studies to understand this shallow active region, in which the largest known earthquake (less than 10 km depth) took place on 4 September 1958 (*M* = 6.9; Lomnitz 1961; Piderit 1961). This activity is probably the surface consequence of the change in dip angle with which the subducting Nazca Plate underthrusts (flat subduction) beneath the South American Plate (Gutscher 2000b).

Large events and characteristics of the seismogenic region

The large Chilean earthquakes have inevitably commanded the most attention since seismicity began to be recorded in the country (Silgado 1985). Only recently, in the last couple of decades, has a significant effort towards understanding the fine structure of the Chilean seismogenic zone materialized. The advancement in quantity and quality of instruments of global networks and the deployment of permanent and temporary local and regional networks has been the key to elucidating the

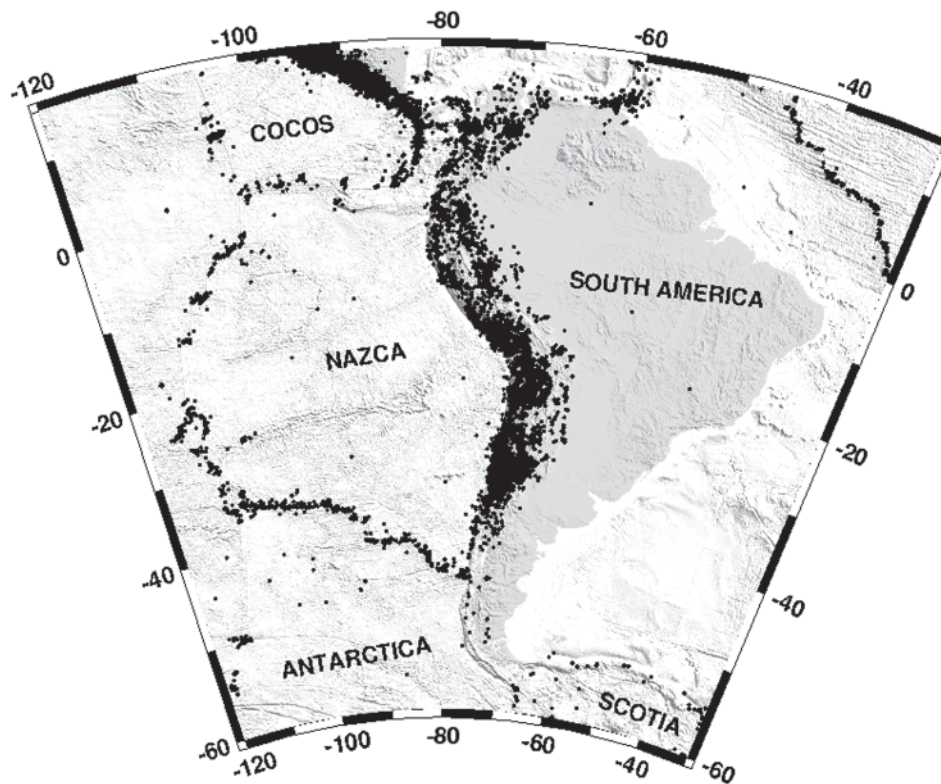


Fig. 10.1. Seismicity defining the Nazca (NA), Cocos and parts of the Antarctic (AN) and South American plates (SA). South of 45°S the Antarctic plate Subducts beneath the SA plate. South of 53°S the situation is more complex because the Magallanes Fault Zone separates the Scotia Plate from the SA Plate. Note the seismic activity decrease to the south of the triple-junction (NA–SA–AN). Figure based seismicity reported by NEIC for the period 1973–2004.

detailed knowledge of the geometry of subduction zones (Wadati–Benioff) and their characteristics such as earthquake focal mechanisms, state of stress, coupling extent, and presence of double seismic regions.

The first systematic seismological effort in Chile was initiated in the first decade of the twentieth century after the occurrence of the significant 1906 Valparaíso earthquake. The government of President Pedro Montt decided to invite Ferdinand Montessus de Ballore (1889–1923) to initiate seismological work in the country. Parts of his plans are reflected in the first page of the first issue of the *Bulletin of the Seismological Society of America* (1911) which includes a map of the existing seismic network in Chile (Fig. 10.4). This network includes a central station in Santiago comprising a two-component horizontal Wiechert pendulum weighing 183 kg and a vertical one with a mass of 163 kg, two 100 kg Bosch-Omori pendulums and an 850 kg Stiattesi two-component pendulum. Four stations of second order in Tacna (now part of Peru), Copiapo, Osorno and Punta Arenas completed the National Seismic Network, each of them equipped with a one-component horizontal Wiechert pendulum of 200 kg. To detect local earthquakes, 29 Agamennone seismoscopes (pendulums recording on curved smoked glass) were distributed across an equal number of locations along the country.

Another major contribution of Montessus de Ballore was his summary work on the seismic history of the region published in several volumes between 1911 and 1916, depicting in detail the major earthquakes and tsunamis which took place before the time of his writings. Perhaps the first regional-scale effort was that initiated by the Carnegie Institution of Washington in northern Chile in the 1960s with the installation of five

instruments inland from Antofagasta. One of the first local systematic efforts in central Chile was the study of the aftershocks of the MW=8.1 event in Central Chile which took place in March 1985 (Comte *et al.* 1986). After this study, not only the characteristics of the aftershocks of the 1985 event were recorded and analyzed, but some of the first tomography studies in Chile were carried out after a wealth of data were acquired by means of a permanent seismic network complemented by a temporary network of seismographs (Comte *et al.* 1986; Pardo *et al.* 2003a). The current seismographic network at the beginning of the twenty-first century is depicted in Figure 10.4. These instruments are mainly composed of short-period sensors and 16-bit digitizers. A few stations around Santiago include broadband sensors with 24-bit digitizers. The stations located in Iquique (IQQ), Calama (LVC), Easter Island (RPN), Las Campanas Observatory (LCO) at the latitude of the city of La Serena, Peldehue (PEL) and Coihaique (COI) are part of international networks such as IRIS, GEOSCOPE and GEOFON, and the National Seismological Service, presently part of the University of Chile in Santiago, regularly publishes seismic activity occurring in central Chile.

Permanent and temporary seismic networks have been deployed from coast to cordillera, in collaborative efforts among different institutions, from north to south covering almost the entire territory. These studies have permitted not only the characterization of the three-dimensional velocity structure of the region, but have also allowed attenuation studies and a clear definition of the seismogenic zone. A comprehensive report of these efforts is summarized below, depicting the underthrusting characteristics of the earthquake mechanisms of very large earthquakes (Fig. 10.6).

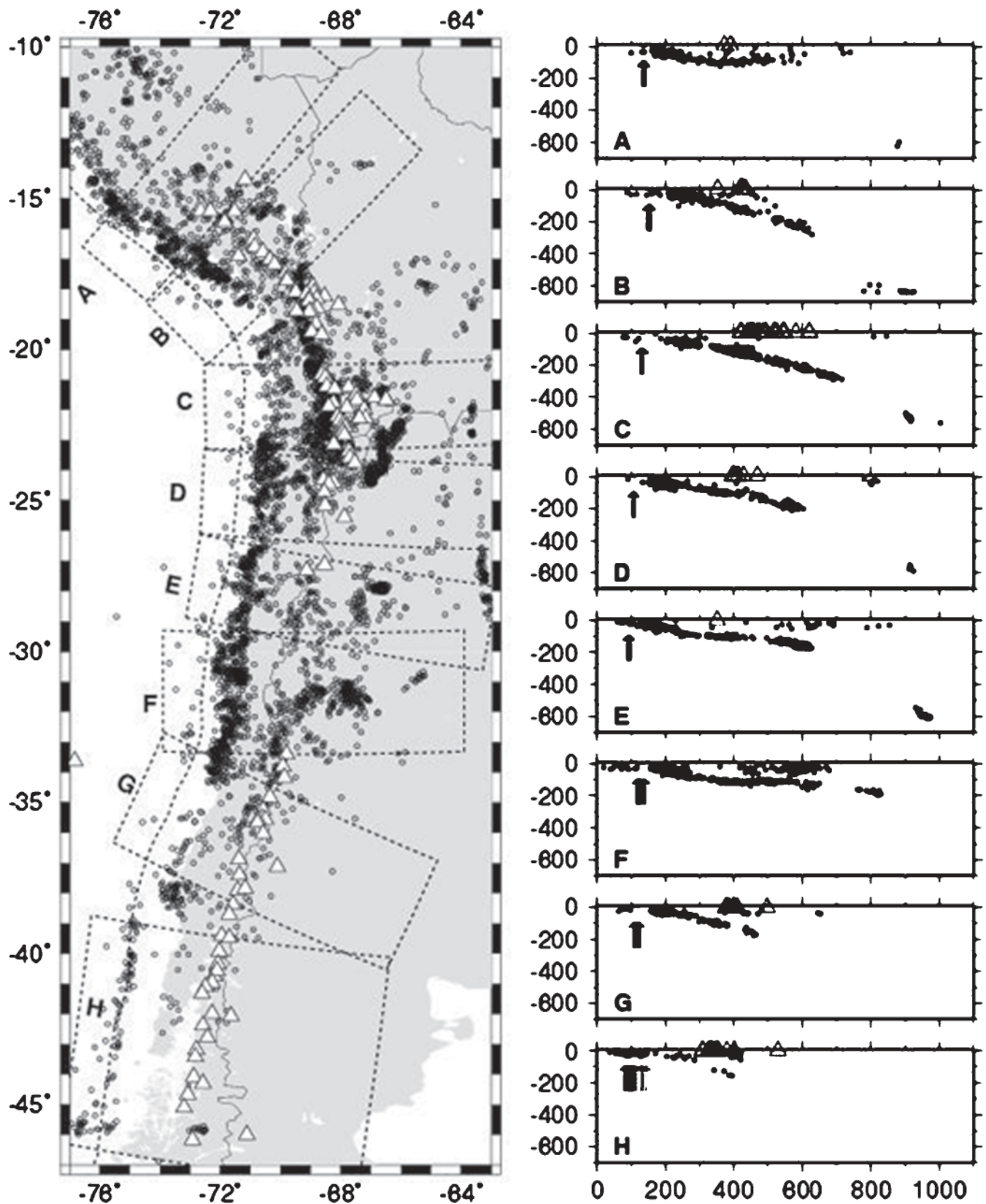


Fig. 10.2. Relocated seismicity (black open circles) on the western flank of South America (Engdahl & Villaseñor 2003). Eight profiles show how the seismicity changes with depth as a function of distance from the trench (upward-pointing arrows, right panels) revealing the different behaviour of the Nazca Plate after subduction and the response of the overriding South American Plate in terms of shallow seismicity. The triangles represent Quaternary volcanic edifices.

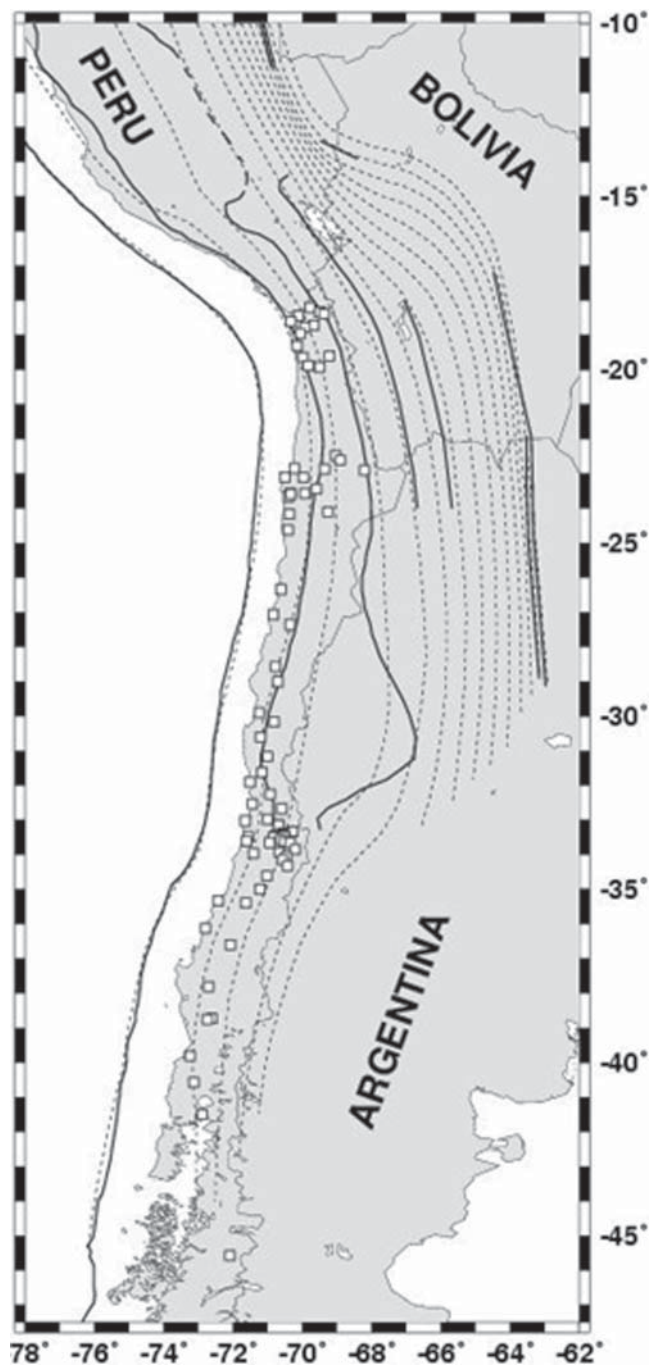


Fig. 10.3. Dashed and solid lines represent contours of equal seismic depth according to Gudmundsson & Sambridge (1998) from 0 to 650 km, every 50 km, and Engdahl & Villaseñor (2003) at depths of 0 (trench), 75, 125, 200, 275, 550 and 600 km. The small squares represent the locations of seismic stations of the Seismological Network of Chile as of 2005. Network efforts around 18°S and 23°S are academic collaborations between the University of Chile and French institutions.

Arica–Tocopilla (17–22°S)

Very large earthquakes have taken place historically in this region, among them the most recent underthrusting event corresponds to the 1877 $M_T=9.0$ earthquake, where M_T is the tsunami magnitude. A rupture zone of nearly 450 km (Kausel & Campos 1992) produced a large tsunami that flooded most of the coastal cities in the area. Significant subsidence was observed along the coast near Iquique and Alacran Island



Fig. 10.4. Seismic Network of Chile as presented by F. Montessus de Ballore after the occurrence of the 1906 Valparaíso earthquake (*Bulletin of the Seismological Society of America*, 1911).

(which is now a suburb of Arica). In his evaluation of earthquake potential along the circum-Pacific belt, Nishenko (1985) categorized this region as a seismic gap, together with the region south of Antofagasta, earlier identified by Kelleher (1972). The southern part of this region—Mejillones Peninsula to Paposo—was reactivated in 1995 with a moment magnitude $M_w=8.0$ event, described in the next section. On the northern extreme of this region, an $M_w=8.4$ earthquake took place in southern Peru in June 2001, which is considered the gap-filling event of most of the area subjected to the effects of the 1868 $M_T=9.0$ (tsunami magnitude; Abe 1979) earthquake (Fig. 10.6). The rupture region of the 2001 event extended for 320 km up to the coastal location of Ilo in southern Peru, about 150 km north of the Arica bend (Giovanni *et al.* 2002). As is the case in most of the studied large events, the rupture propagated mainly from north to south (Beck *et al.* 1998).

These two very large shocks that took place in the nineteenth century, in particular the 1868 event, which was felt from Guayaquil (Ecuador) to Valparaíso, did not go unnoticed. The

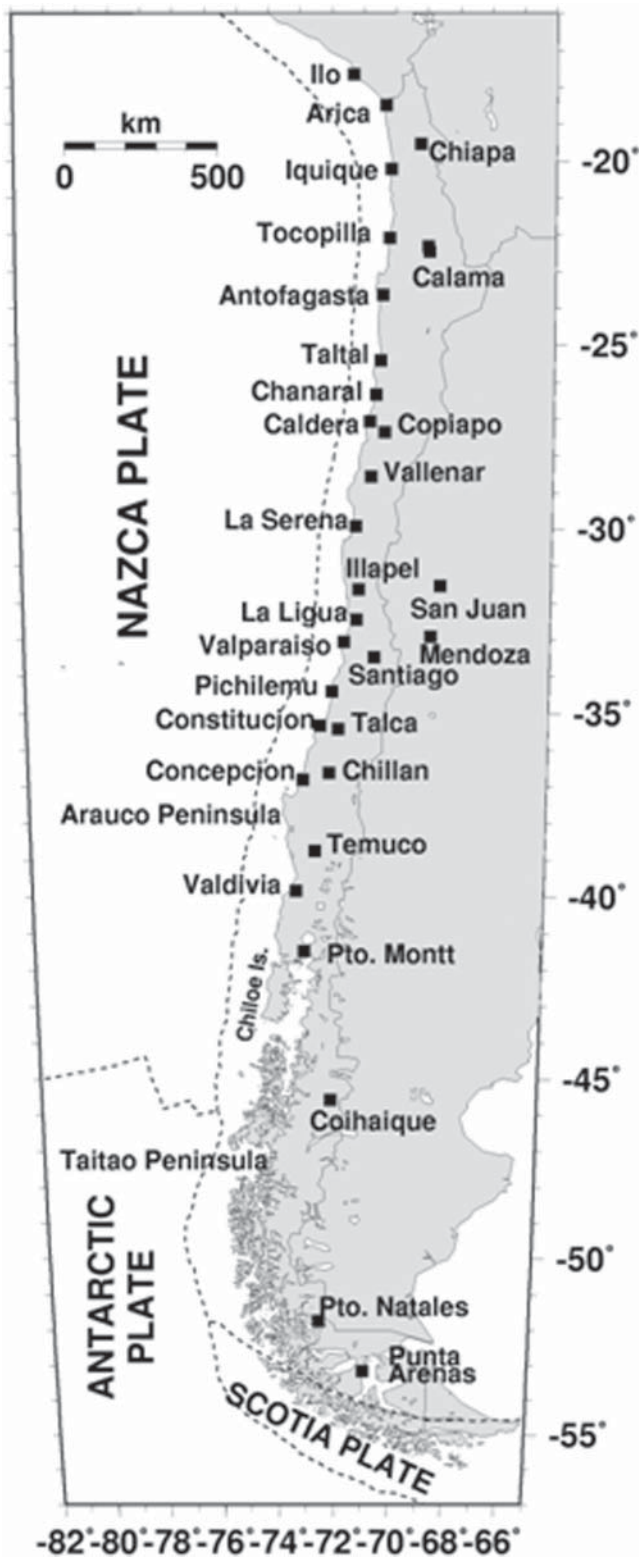


Fig. 10.5. Names of cities and places mentioned in the text. Most of these cities, up to 46°S in the south, have been subjected to the devastating effects of large earthquakes.

city of Arica was severely damaged by ensuing tsunamis which reportedly reached runups of up to 15 m (Lockridge 1985). Analysis of the arrival times of the tsunamis at different locations along the coast, along with the characteristics of the runups for the 1868 and 1877 events, allowed Díaz (1991) to

estimate maximum rupture lengths of 680 and 510 km with corresponding displacements of nearly 14 and 10 m, thus the estimated magnitudes M_w would be 9.0 and 8.9, respectively, both significantly larger than those presented by Kausel & Campos (1992). The southern extreme of the 1868 rupture reached beyond the Arica bend, farther to the south than the dislocation associated with the recent 2001 event. Thus, a stretch of nearly 500 km along the coupled region of southern Peru–northern Chile (Ilo–Arica–Mejillones Peninsula) has not been subjected to significant earthquakes since 1868–1877. Comparison of tsunami amplitudes recorded in Japan, at Hakodate, indicate maximum values reaching 2 m (Soloviev & Go 1984) and 3 m (Lockridge 1985) for the 1868 event compared to maximum values of 1 m for the 2001 event.

Comte & Suárez (1995) and Comte *et al.* (1999) characterized the initial dip angle of the Wadati–Benioff region at 20°E and confirmed that this region also represents a double seismic region as has been observed in other subduction environments. Relatively large extensional events (normal faulting) within the subducting Nazca Plate, with hypocentres beneath the coast, have taken place recently, the event of 8 August 1987 (18.96°S, 70.02°W) with $M_w = 7.2$ at 80 km depth being the largest and most recent example (Fig. 10.7).

David *et al.* (2005) reported on crustal seismicity in the forearc of Arica as registered by several temporary seismographic deployments in addition to the southernmost stations of the Peruvian National Network and the permanent network of Arica, installed in 1994. A possible association of shallow seismicity with the Incapuquio Fault System (southern Peru) is reported, and the Copacilla–Tignamar Thrust and Fold Belt (in northern Chile) might also be involved. These two systems form the limit between the Pacific Piedmont and the Western Cordillera. Farther to the south, a relatively large ($M_w = 6.3$) shallow event took place with its epicentre below 19.44°S, 69.18°W at a depth of 15 km (see Fig. 10.7). The Harvard moment tensor solution can be interpreted as a right-lateral displacement on a north–south plane dipping 46°E. This is an unusually large magnitude for a shallow event in the region.

Another important source of seismic activity is the region where the top part of the subducting plate reaches about 100 km depth and undergoes normal faulting, as was the case for the 13 June 2005, $M_s = 7.9$ event (20.02°S, 69.17°W) at 95 km depth. This event caused severe destruction in the towns and villages in the epicentral area, near Chiapa (Fig. 10.7).

Antofagasta–Taltal (22–25°S)

The 1995 Antofagasta earthquake, $M_w = 8.1$, which extended from Mejillones Peninsula to Papos, is probably the best studied earthquake in Chile to date. Ruegg *et al.* (1996) presented the first characterization of the earthquake based on repeated Global Positioning System (GPS) observations and inversion of seismograms at teleseismic distances. GPS measurements indicated that the southern part of Mejillones Peninsula was uplifted about 15 cm, the city of Antofagasta itself was in a nodal axis (no vertical change) and maximum subsidence (34 cm) took place just inland behind Cerro Paranal, the highest point in the region, at 2635 m above mean sea level. Maximum horizontal displacement reached about 0.8 m to the WSW with respect to the easternmost observation point of the profile. Klotz *et al.* (1999) reported on 70 repeated GPS measurements observed in the area affected by the 1995 event. According to these observations, the city of Antofagasta was shifted 80 cm westward and horizontal displacements reached 10 cm as far as 300 km away from the trench. Another interesting result of their study is that the slip angle (rake) was 66°, implying that the oblique convergence between the Nazca and South American plates is accommodated by oblique convergence slip, not by slip partitioning. Additionally, they observed that the present-day crustal shortening of 3–4 mm/year is much slower than the average value of 8–14 mm/year for

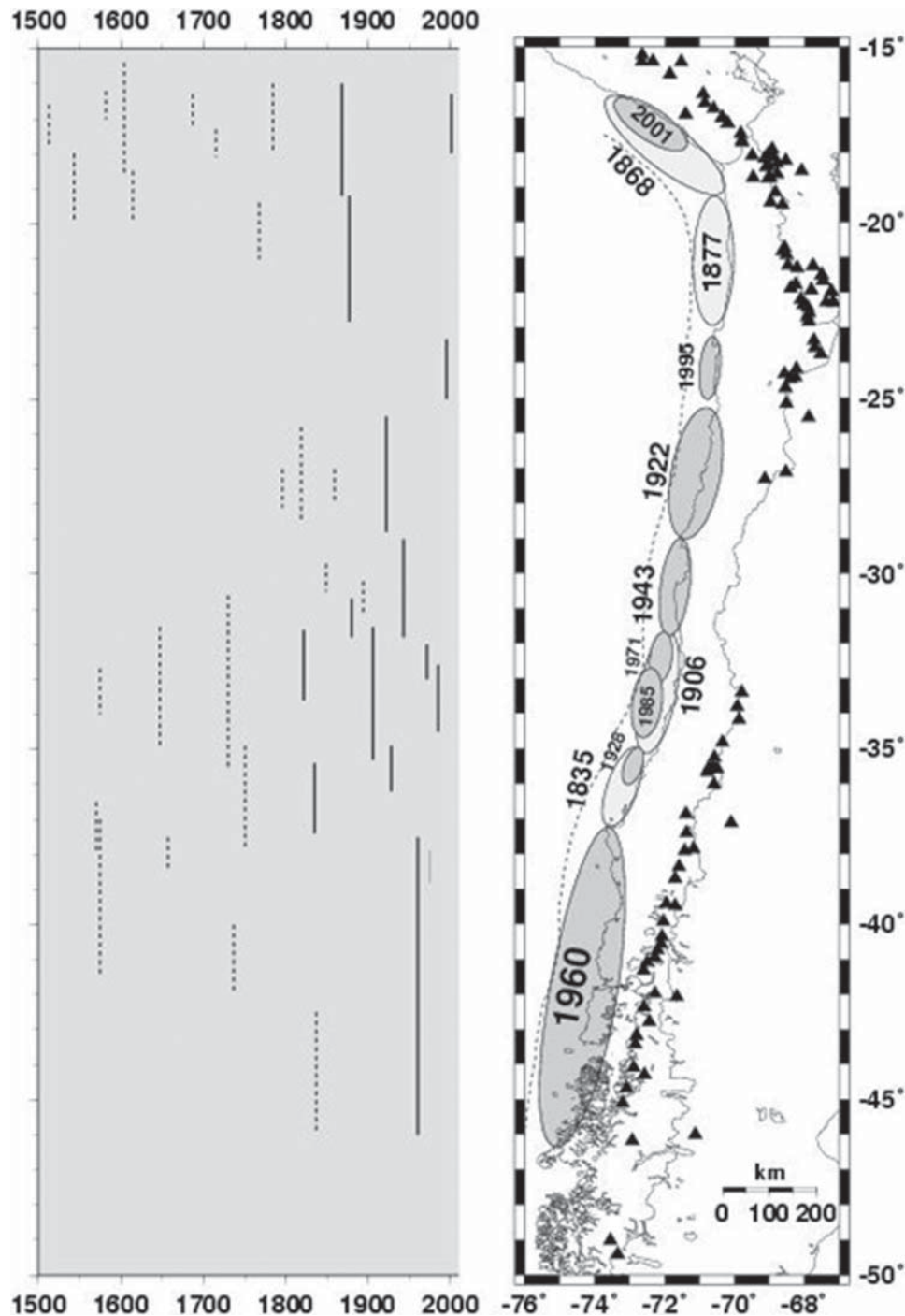


Fig. 10.6. Rupture lengths of large earthquakes in Chile in the past 500 year (left panel). Continuous lines indicate rupture zones better constrained than those represented by dashed lines. Ellipses (right panel) mark roughly the rupture zone of the most recent significant events along the coasts of southern Peru and Chile. The dashed line represents the trench axis and the black triangles are Quaternary volcanoes.

the last 27 million years. A continuous GPS instrument placed in the southern part of the city of Antofagasta showed no precursory displacement or immediate post-seismic adjustments (Klotz *et al.* 1999). Additional indicators of elevation changes along the coast were provided by Ortlieb *et al.* (1996) on the basis of death of coralline algae (lithothamnium) in the intertidal environment. As this coralline alga dies its colour turns from pink to white, leaving an infralittoral fringe, which depends on the amount of elevation; this had a maximum thickness of 80 cm at the southwestern tip of the Mejillones Peninsula, while

the coast at Antofagasta suffered practically no vertical change, in agreement with repeated GPS observations. Coastal uplift is noticeable, about 10 cm, again about 100 km south of Antofagasta (near Punta Tragagente). The preferred solution of Ruegg *et al.* (1996) involves a 180-km-long rupture on a plane dipping between 19° and 20° to the east. The source time function comprised three main pulses propagating southward; the main pulse of moment release (second) coincides with the location of the Harvard centroid calculated by Dziewonski *et al.* (1996).

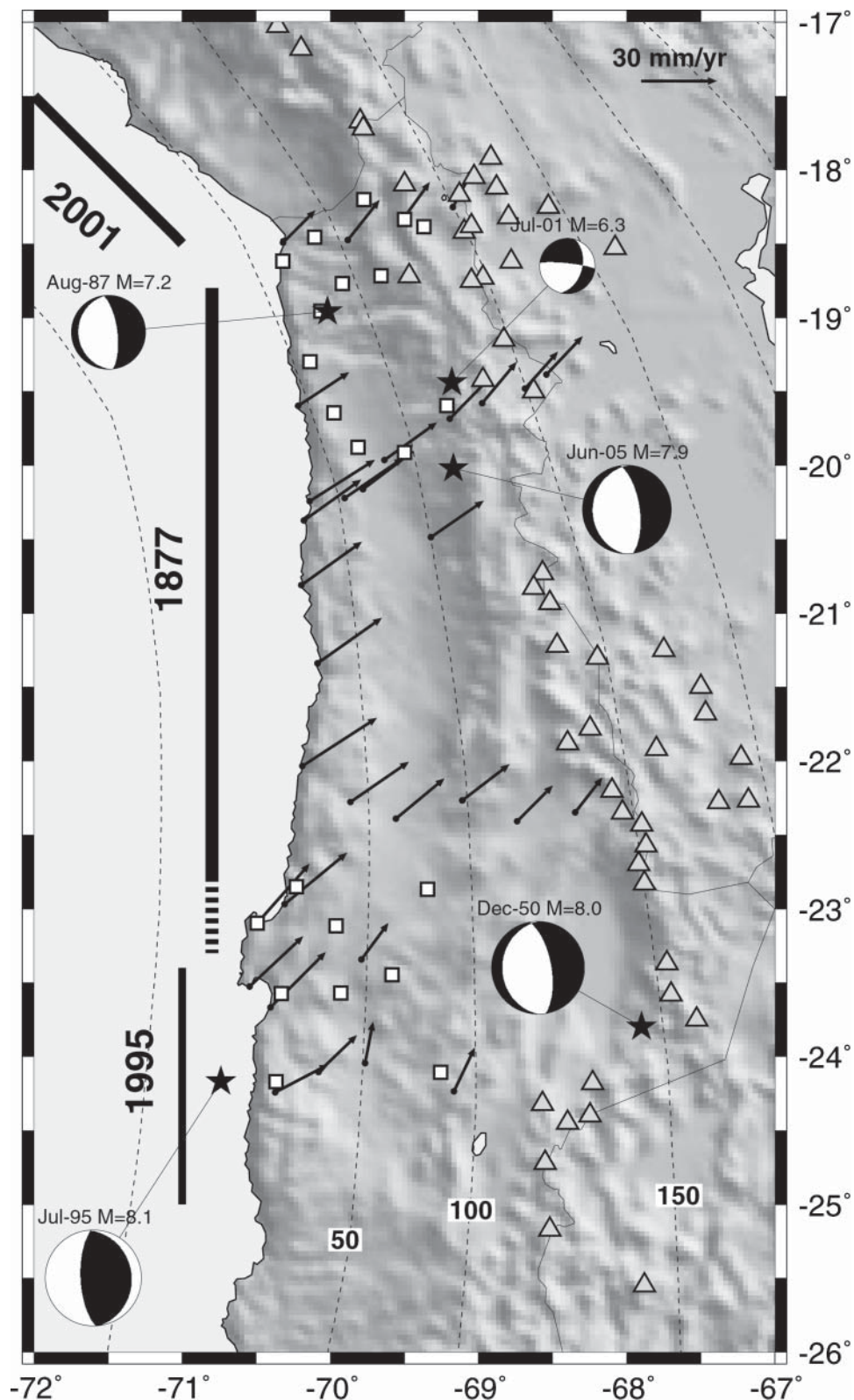


Fig. 10.7. The estimated rupture zone (it is not known whether the Mejillones Peninsula participated, hence the dashed line) of the 1877 great earthquake lies between the sites of the $M_w = 8.0$ July 1950 Antofagasta and the $M_w = 8.4$ June 2001 southern Peru earthquakes. Three large normal-fault-type (tensional) earthquakes took place in 1950 ($M = 8.0$), 1987 ($M = 7.2$) and 2005 ($M = 7.9$). Earthquakes, such as the one of July 2001 ($M = 6.3$) at 15 km depth, at the western flank of the Andes, are not reported very often but it is clearly consistent with what has been observed further to the south, in the Precordillera at the latitude of Antofagasta. Volcanoes are open triangles and GPS observations (1996–1999; Chlieh *et al.* 2004) indicate shortening rates of the order of 30 mm/year at the coast.

Delouis *et al.* (1997), using data collected from a permanent network around Antofagasta complemented with additional temporary instruments, reported on a study of aftershocks within the context of this area experiencing a possible precursor to the impending earthquake in northern Chile (which now corresponds to the southern extension of the 2001 Arequipa earthquake and the northern extreme of the 1995 Antofagasta event, 23°S; see Fig. 10.7). These authors also reported on the peak ground acceleration of 0.28 g in the east–west component of a strong ground-motion sensor recorded in the city of Antofagasta. Subsequently, Graeber & Asch (1999) and Husen *et al.* (1999, 2000) studied the velocity structure of the region around the 1995 event, using both aftershocks of this event as well as regularly occurring events by means of offshore and inland networks, giving rise to one of the most detailed views of three-dimensional velocity variations and location of aftershocks for any event in Chile (Fig. 10.8). Geometrical definition and characterization of the seismogenic zone, from 20 to 46 km depth along the Wadati–Benioff zone, were among the main results of these studies. Figure 10.9 shows the two profiles, north and south of 23°S, both defining the Wadati–Benioff zone as well as an important shallow seismicity (Graeber & Asch 1999), part of which is displayed in Figure 10.10 (Belmonte 2002).

Interferometric Synthetic Aperture Radar (InSAR) was recently developed as a tool to determine the distance along the line of sight from radar satellites. Repeated observations give

an estimation of the changes in distance. The first applications of InSAR to earthquake and fault monitoring in Chile have been the works of Pritchard *et al.* (2002) and Chlieh *et al.* (2004) on the 1995 earthquake. While the first study emphasizes the analysis of the coseismic displacement field, the second study concentrates on the evaluation of the post-seismic displacements. In their study, Pritchard *et al.* (2002) recover the whole ‘coseismic’ displacement field (combination of images taken in 1992 and 1997). The results of their work are consistent with other estimations of the order of 5 m for coseismic displacement (Ruegg *et al.* 1996; Ortlieb *et al.* 1996; Ihmlé & Ruegg 1997). One of the major outcomes of their study is that, at a resolution of few centimetres, no displacement was observed along the Atacama Fault segment just above the active portion during 1995. The Atacama Fault is a major feature that extends from south of Iquique at 22°S in its northern extreme to around 25°S, close to Taltal, and bounds the Coastal Cordillera on its eastern flank. Arabaz (1968, 1971) unsuccessfully tried to find displacement along the Atacama Fault associated with the December 1966, $M_s = 7.8$ Taltal earthquake.

In addition to the InSAR information, Chlieh *et al.* (2004) used the difference of GPS positioning along 40 benchmarks measured between 1996 and 1999 to refer the InSAR fringes to a known displacement field. They interpreted the observed surface deformation as mostly the result of aseismic slip along the down-dip extension (transition zone) from 35 km to 55 km depth as well as post-seismic displacement in the northern

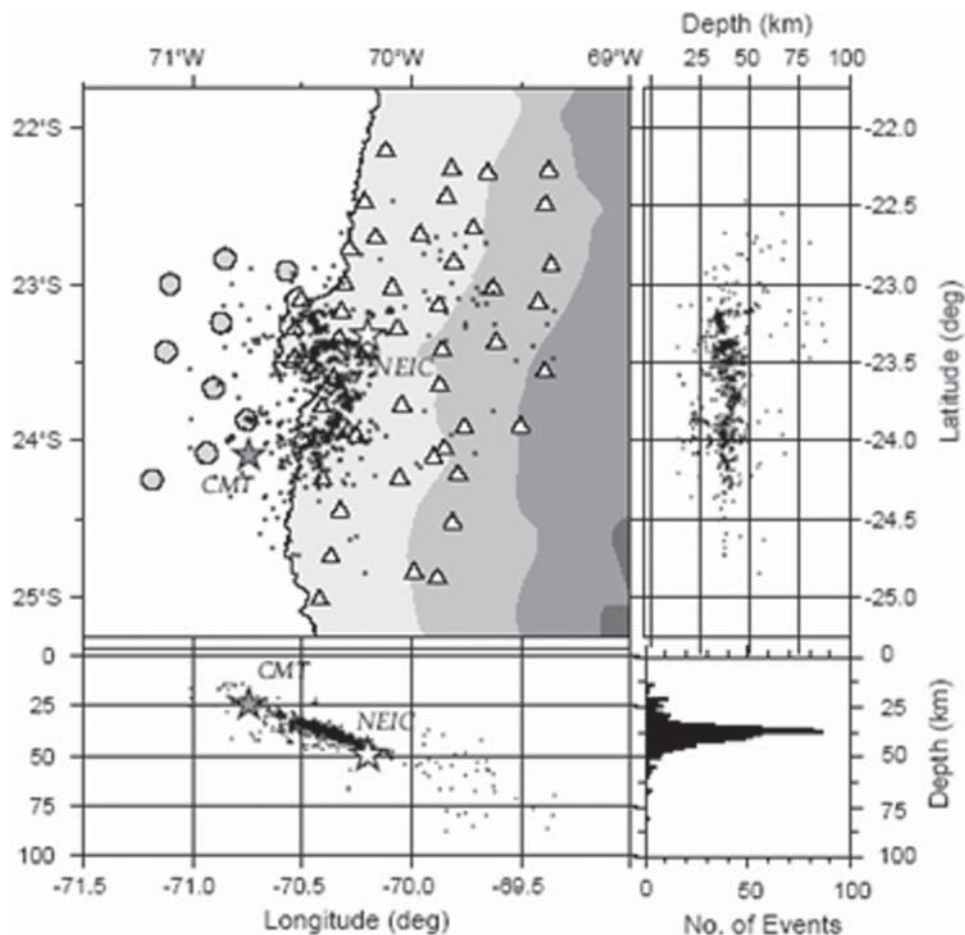


Fig. 10.8. Hypocentral distribution of 789 well-located events (after Husen *et al.* 2000). Lower left shows an east–west cross-section and upper right shows a north–south cross-section. Stars mark the hypocentre determination of the Antofagasta earthquake by NEIC and Harvard CMT, indicating a southward rupture. The rupture extended roughly from 23.4°S to 25.0°S. At the lower right corner a histogram depth distribution is shown. Triangles and circles denote on- and off-shore stations.

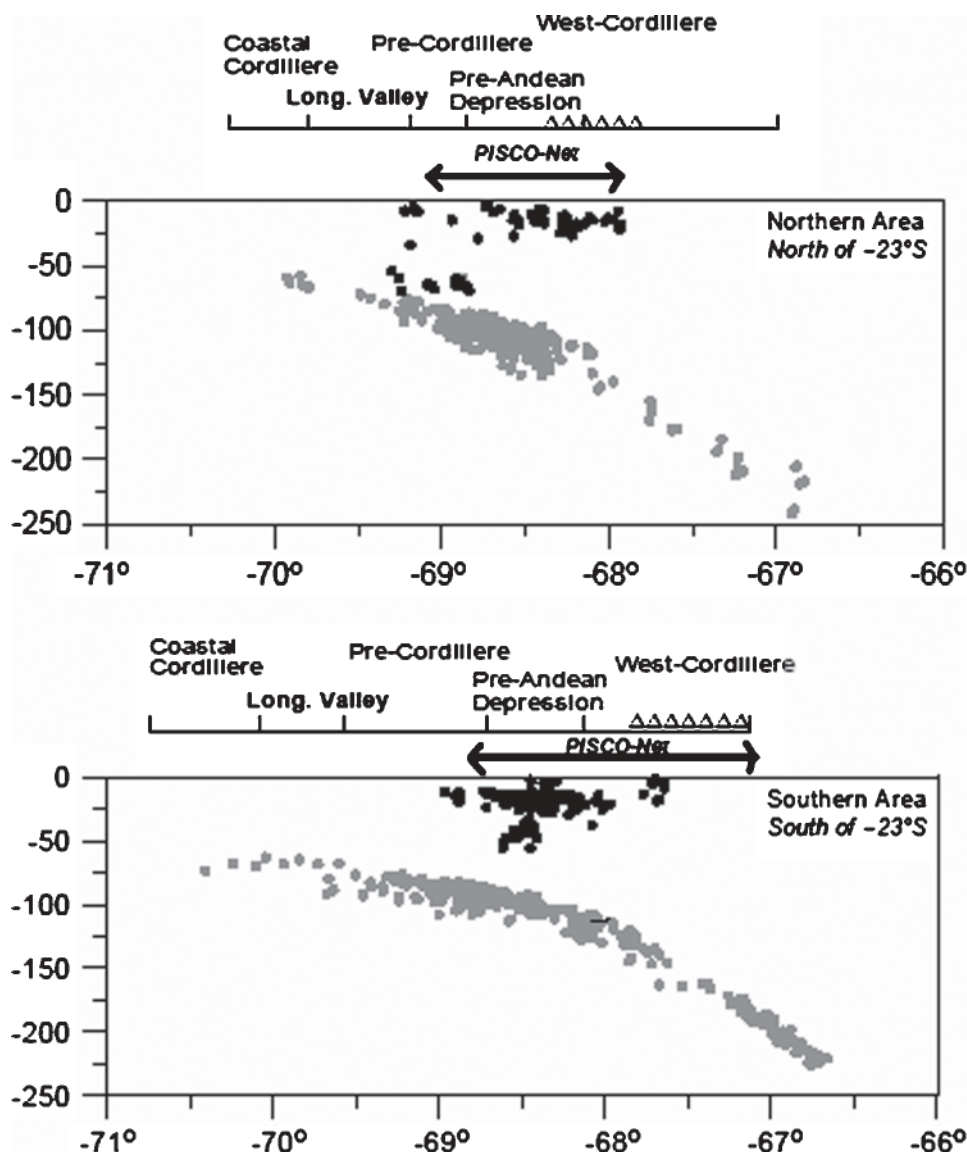


Fig. 10.9. Distribution of crustal seismicity (black points) north and south of *c.* 23°S. Grey points refer to PISCO data (Graber 1997) and Wadati–Benioff zone seismicity. Figure from Belmonte *et al.* (2006).

lateral extension of 25–45 km, under the Mejillones Peninsula, a prominent geomorphological feature just NW of Antofagasta. There is general agreement that this is the southern limit of the 1877 rupture (Delouis *et al.* 1997; Chlieh *et al.* 2004).

As was the case in the region to the north, extension occurs further along the subduction zone. A significant extensional event ($M_w = 8.0$) took place in December 1950 at 100 km depth near the city of Calama (Kausel & Campos 1992). The mode of rupture of this event has been interpreted as a normal fault rupturing the whole Nazca Plate, initiating at 100 km depth and extending downward.

As has been the case in the Arica region, Kono *et al.* (1985) examined the unusual east–west orientation of the compressive field for the 17 January 1977 earthquake (24.9°S, 68.7°W). They proposed, because of its depth at 120 km, that it might be indicative of a double Benioff zone. Many tomographic as well as velocity–structure studies have been carried out in this region utilizing mainly the aftershock of the 1995 event as well as regular seismicity (Haberland & Rietbrock 1998; Ancoorp Working Group 1999; Schmitz *et al.* 1999; Graeber & Asch 1999; Bock *et al.* 2000).

Copiapó (26–29°S)

Farther to the south is the Copiapo region, a site of major earthquakes in 1819 and 1922. Lomnitz (2004) reported that the 1819 event had two large foreshocks, on 3 and 4 April. The main event, of magnitude 8½, on 11 April, was felt over a radius of 800 km and caused a major tsunami which destroyed the port of Caldera. According to Lockridge (1985), the 1922 earthquake generated a local tsunami with maximum wave heights of 9 m and a farfield amplitude in Japan of 39–70 cm. Kelleher (1972), from the analysis of the aftershocks recorded in La Paz, Bolivia, deduced a rupture extension of about 470 km in a north–south orientation. Willis (1929), in the spectacular report of his field expedition to study the 1922 event, reported that the towns of Copiapo, Vallenar and La Serena were among the most severely damaged. Three main shocks within the first few minutes were reported by local residents of Copiapo, Vallenar and La Serena, hence Willis concluded that the 1922 earthquake was the result of three events with different epicentres; this is further verified by Beck *et al.* (1998) when analysing the first 75 s of the P-wave train in which three main pulses

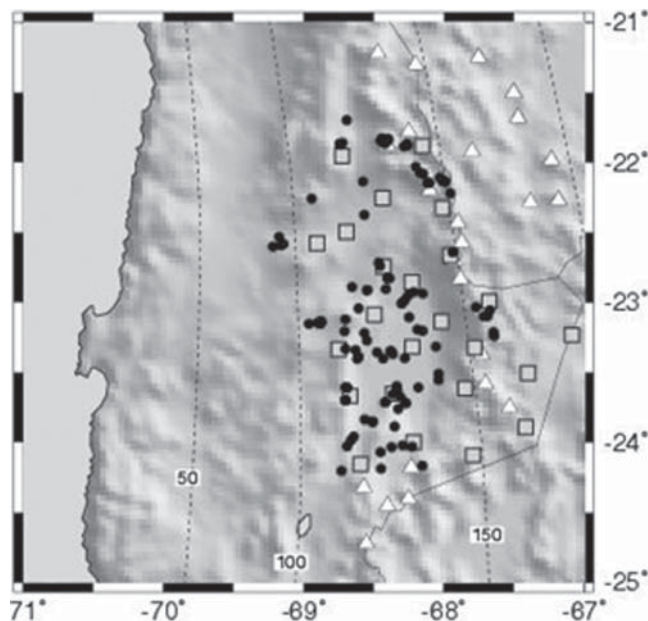


Fig. 10.10. Distribution of crustal seismicity after Belmonte (2002). Dark circles are shallow events (0–20 km depth) and grey squares represent locations of stations used during the PISCO experiment. The majority of the shallow seismic activity is located in the western boundary of the volcanic chain as well as in the Precordillera Fault System and the Salar de Atacama. Open triangles represent Quaternary volcanoes.

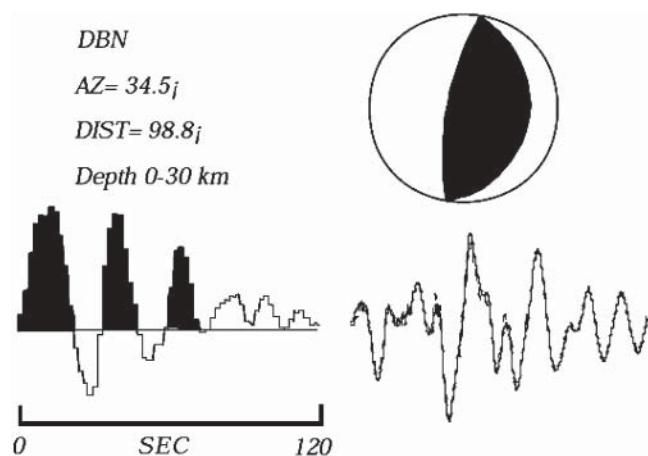


Fig. 10.11. Three main pulses (75 s) of the source time function of the November 1922 derived from the P-waveform recorded at De Bilt, the Netherlands (DBN). Solid and dashed lines represent the observed and modelled signals, respectively. The focal mechanism was derived from P-wave first motions (Beck *et al.* 1998).

are observed in the inversion for the source time function (Fig. 10.11). The northern part of the 1922 rupture zone was partially reactivated in 1983 with an event of $M_w=7.8$ (Dziewonski *et al.* 1983), with hypocentre at 38 km producing a minor tsunami. Beck *et al.* (1998) proposed that the 1922 segment failed in multiple-asperity-type rupture. A heterogeneous style of faulting in the 1922 rupture zone is further suggested by the occurrence of two previous earthquakes in 1796 and three in 1819. The evidence thus implies that this region does not always fail in a single rupture, but at least sometimes the energy is released in clusters of medium to large events.

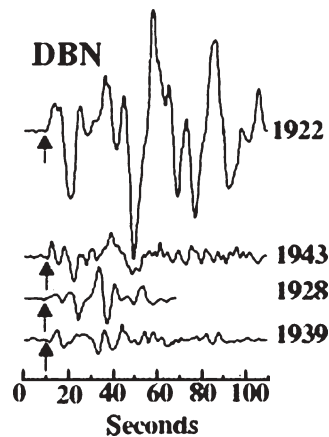


Fig. 10.12. P-waveforms at station DBN (De Bilt, the Netherlands) of the 1922 (Dist = 99°), 1943 (Dist = 101°), 1928 (Dist = 104°) and 1939 (Dist = 105°) earthquakes. Observe the difference in amplitude between the 1922 Copiapo event and the rest.

Comte *et al.* (2002) analysed a two-month period of data recorded during a deployment of on- and offshore instruments carried out in 2001. Consistent with other studies, the Wadati–Benioff zone in the coupled region (thrust interplate contact that generates large events) has an average dip angle of 20°, the same as that derived for other regions of Chile.

La Serena–La Ligua (30–33°S)

P-waves recorded at teleseismic distances are consistent with an underthrusting mechanism for the 1943 Illapel $M_w=7.9$ event (Beck *et al.* 1998). This earthquake is much smaller and simpler than that of 1922 (see Fig. 10.12). A single pulse of duration 24–28 s for a time function on a source with a shallow dip to the east satisfies well the constraints of the teleseismic waveforms (Beck *et al.* 1998). As is characteristic of the largest underthrust earthquakes in Chile, a local tsunami, which damaged some fishing boats at Los Vilos, was observed along the coast. The farfield tsunami in Japan reached maximum amplitudes of 30 cm (Lockridge 1985). Kelleher (1972), based on aftershock S–P times recorded in Bolivia, estimated the extent of the rupture zone to be about 360 km.

In October 1997, a $M_w=7.1$ intraplate earthquake took place at roughly 31°S, 71.2°W, very close to the town of Punitaqui. Apart from the significant damage produced in the closest towns, the most important characteristic of this event is that it was the result of a nearly vertical fault with rupture initiation at 68 km depth, probably a result of the unbending of the Nazca Plate when reaching subhorizontality to the east of 70.5°W (Pardo *et al.* 2002b). Lemoine *et al.* (2001) interpreted this downward rupture as the result of down-dip compression. Choy & Kirby (2004) calculated an apparent stress drop τ_a ($\tau_a = \mu E_s / M_0$, where μ is rigidity; E_s is the radiated energy; and M_0 is the moment of the earthquake.) of 4.4 MPa (44 bar) for this event, the largest in the suite of all normal faults worldwide between 1987 and 2001.

Prompted by the study of two significant earthquakes in 1965 ($M_s=7.1$, $mb=6.4$) and 1971 ($M_s=7.5$, $mb=6.6$, with M_s being the surface-wave magnitude and mb the body-wave magnitude) near the town of La Ligua, on the northernmost extension of the 1906 event, Malgrange *et al.* (1981) concluded that shallow underthrust events and deeper tensional-type events coexist along the coast from southern Peru to central Chile. Both events produced roughly the same peak ground acceleration in Santiago (0.19g and 0.17g). Additionally, in their comparison of these two events, Malgrange *et al.* (1981) point to the lower stress drop of the 1971 underthrusting earthquake (3.8 MPa or 38 bar) in comparison with the 9.1

MPa (91 bar) of the 1965 tensional event. This point was later used by Kausel & Campos (1992) to generalize that interplate normal fault mechanisms usually have larger stress drops and produce important damage in the cities of the central valley. This point is of utmost importance when the 1939 Chillán, farther south, event is considered (see below for the Pichilemu–Concepción region).

The region between 27°S and 33°S is characterized by the southward gradual decrease of the dip angle of subduction, the absence of a central valley between the Coastal Cordillera and the Andes and lack of recent volcanism, unlike to the north of 26°S and south of 33°S. These changes in the dip angle are only noticeable when the upper part of the subducting Nazca Plate reaches a depth of about 100 km. Therefore the initial part of the subduction (0–50 km) has similar characteristics from Arica (18.5°S) to Taitao (46°S) regarding the inclination of the subduction plate. Gutscher *et al.* (2000b) proposed that the flat subduction is caused primarily by the buoyancy effect of anomalously thick (15–20 km) subducted oceanic crust.

Tomography studies in the transition from flat-slab subduction to normal subduction (north and south of 33.5°S, respectively) indicate that the mantle conditions vary significantly; Wagner *et al.* (2005) postulate that the low P-wave, low S-wave velocities and high Vp/Vs ratios to the south of 33.5°S are an indication of localized pockets of melt. In contrast the low P-wave, high S-wave velocities and low Vp/Vs ratios reflect the absence of melt mineralogies to the north of 33.5°S, indicating the absence of an asthenospheric wedge to create the adequate conditions for active volcanism to develop.

Valparaíso–Pichilemu (33–35°S)

This is the region with the longest historic earthquake record in Chile because it was part of the first settlements of the Spanish conquerors, who kept written records after 1541, when the city of Santiago was founded, with Valparaíso being its main sea-port.

The earthquake in central Chile on 3 March 1985 corresponds to the last example of the sequence that has been taking place regularly in the region every 82 ± 6 years. The events that constitute the sequence 1647, 1730, 1822, 1906 and 1985 present several common features: offshore epicentre location, rupture lengths of over 150 km, systematic coastal uplift and small tsunamis compared to the size of earthquakes, with the possible exception of the tsunami associated with the 1730 event. Although the recurrence intervals have been very regular, the rupture lengths differ substantially; the largest rupture, close to 600 km, was that associated with the 1730 event (Comte *et al.* 1986; Barrientos & Kausel 1988). Lomnitz (2004) has argued that the epicentre of the first recorded earthquake in this sequence, in 1647, might have been inland, either in the High Andes in a similar manner to the 1958 shallow event, or in what has been recently recognized as the San Ramon Fault (Rauld 2002). The San Ramon Fault trends north–south along the western flank of the Andean foothills, along the easternmost limit of the city of Santiago. However, detailed seismic monitoring of the Santiago basin during the last 30 years has not provided any evidence of seismic activity along this fault.

One of the first detailed accounts of coastal elevation changes associated with a large earthquake in this region is provided in the journal kept by Mrs Maria Graham (1824) during her short stay on the coast of central Chile. She experienced and witnessed the consequences of the 1822 earthquake, and reported elevation changes of the coast for nearly 160 km, in particular of nearly 1.0 m at Valparaíso and about 1.2 m at Quintero (30 km north of Valparaíso).

Okal (2005) re-evaluated the two earthquakes that took place within 30 minutes of each other on 17 August 1906 in the Aleutian Islands and central Chile, through the analysis of mantle waves; he concludes that the latter was a regular subduction zone event with moment of 2.8×10^{28} dyne-cm and argues that

its size has been overestimated by previous authors, with the exception of Kanamori (1977), and that its rupture length did not exceed 200 km. Steffen (1907) reports coastal uplift from Llico (34.8°S) to Los Vilos (31.9°S), along more than 300 km. These seismically determined smaller coseismic moments can be reconciled with Steffen's coastal observations if we consider an important post-seismic displacement, as was the case of the 1985 central Chile event (Barrientos 1997).

An mb=5.5 foreshock took place about 13 s before the initiation of the 1985 Mw=8.0 earthquake; Comte *et al.* (1986) place both epicentres, at 33.24°S, 71.85°W, $h=17$ km, within the region in which more than 200 precursors took place up to eight days earlier. Christensen & Ruff (1986), based on the deconvolution of P and PP waves, concluded that the rupture took place at depths between 10 and 40 km and the energy was released in two pulses, separated by 16 s, with the second one propagating to the south approximately 75 km away from the first. They also noted that the aftershock region was much larger than the proposed rupture. The mean focal mechanisms coincide with low-angle thrusting events (dip angles around 10° to 20°). Through the study of Rayleigh waves (R1, R2, R3 and R4) recorded at GEOSCOPE and IDA stations, Monfret & Romanowicz (1986) inferred that the rupture of 100–150 km propagated southward or to the SW depending on the type of surface waves used for the analysis. They estimated source time functions of 60–80 s with a moment of 1.2×10^{21} N m (1.2×10^{28} dyne-cm) or Mw=8.0; Zhang & Kanamori (1986) used the spectra of long period waves (150–300 s) to estimate the source longitudinal extent, and they found a 160-km-long rupture orientated on a 10°E azimuth ($M_0=1.2 \times 10^{21}$ N m). Korrat & Madariaga (1986) proposed that the rupture associated with the 1985 event is the continuation of the sequence initiated in July 1971 with an M=7.5 earthquake ($M_0=5.6 \times 10^{19}$ N m).

Precise relocation of the 1985 aftershocks allowed Pardo *et al.* (1986) to conclude that the maximum area involved in the rupture included a region of 200 km by 90 km on a plane dipping approximately 10°E, with most activity within 10 and 45 km depth. Average focal mechanisms coincide with low-angle fault planes. Choy & Dewey (1988) studied the details of rupture initiation and concluded that the earthquake consisted of three stages within 30 s. They also noted that deeper aftershocks showed larger stress drops and their fault dip angles changed to 25–30° when compared to shallow aftershocks (5–10°).

Another interesting feature of this region is the presence of shallow seismicity (<20 km depth) in the Andes (Barrientos *et al.* 2004b). This seismicity extends from the Sierras Pampeanas in Argentina (Alvarado *et al.* 2005) and continues along the Andes to the south (Fig. 10.13). The limit of the southern extension is not well defined because this region lacks the appropriate distribution of sensors to characterize low-magnitude seismicity, but a relatively large (Mw=6.4) event took place in August 2004 on the border between Chile and Argentina (35.17°S, 70.53°W, at 16 km depth) on a N21°E azimuth fault dipping 61° to the east with almost pure right-lateral displacement responding to a mainly WSW–ESW compressive axis. In September 1958 a shallow M=6.9 earthquake took place in Las Melosas, in the Andes along the Maipo Valley, less than 60 km away from central Santiago (Fig. 10.14). This event reached intensity X in the Modified Mercalli Intensity Scale causing landslides which closed the roads and inflicted significant damage to a hydroelectric power plant at Los Queltehues (Lomnitz 1961): the focal mechanisms calculated at that time are presented in Figure 10.14. Six years of shallow Andean seismicity (Fig. 10.14) analysed by Barrientos *et al.* (2004b) show concentrated activity associated with volcanism (panels D and G) together with NW–SE trending features. No surface rupture evidence has been found to be associated with this activity.

Araneda *et al.* (1989) also used a 25–30° dip angle to model the static deformation revealed by repeated measures of over

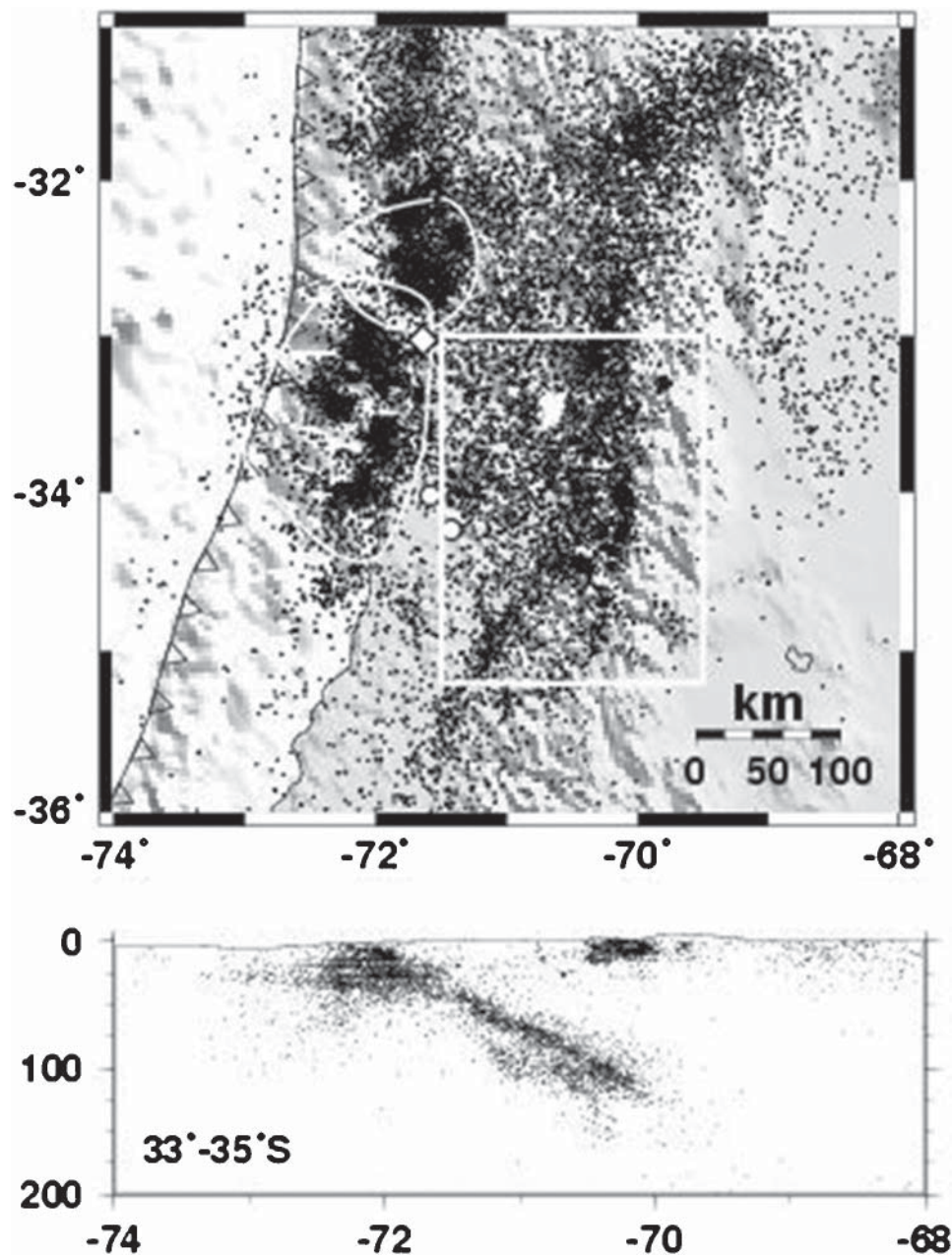


Fig. 10.13. Map (above) and cross-section (below) views of seismicity in central Chile as recorded by the local network between January 1986 to December 2001. Most of the earthquake activity is located along the plate interface as well as within the subducting plate (after Barrientos *et al.* 2004b). The seismicity at shallow depth (0–20 km) within the white box, located on the western flank of the Andes, is expanded in Figure 10.14. The rounded white lines represent the aftershock zones of the 1971 (northern) and 1985 (southern) earthquakes. The small diamond, located at one of the intersections of both lines, represents Valparaíso, where a tide gauge recorded vertical coastal movements; in a similar manner the Rapel Lake (two small white circles) recorded tilt.

a 100-km-long levelling line between Santiago and Algarrobo, located about 100 km away on the coast. Barrientos (1988) estimates the slip distribution from the information provided by the levelling lines, tide gauges at Valparaíso, and two limnigraphs located at the extremes of Rapel Lake, towards the southern part of the rupture region (Fig. 10.15). The latter two observations imply that a significant amount of immediate post-seismic displacement was associated with this event.

As has been the case in other regions, the Santiago area is also exposed to the effects of relatively large intermediate-depth (80–110 km) tensional-type earthquakes. In September 1945 a $M = 7.1$ event took place at 90 km depth which produced a peak ground acceleration of 0.13g (Lepe & Torres 1950) in Santiago

compared to the 0.05g recorded with the same instrument for the 1958 event at a closer hypocentral distance. Barrientos *et al.* (1997) estimated that an earthquake magnitude 7.5 in this intermediate-depth zone could present recurrence periods of approximately 110 years in the region between 32°S and 37°S, generating intensities of the order VIII (Modified Mercalli Scale).

Pichilemu–Concepción (35–37°S)

This part of Chile marks the transition between well-defined seismic zones to the north and south, and has been recognized as a region with moment release deficit (Barrientos 1990;

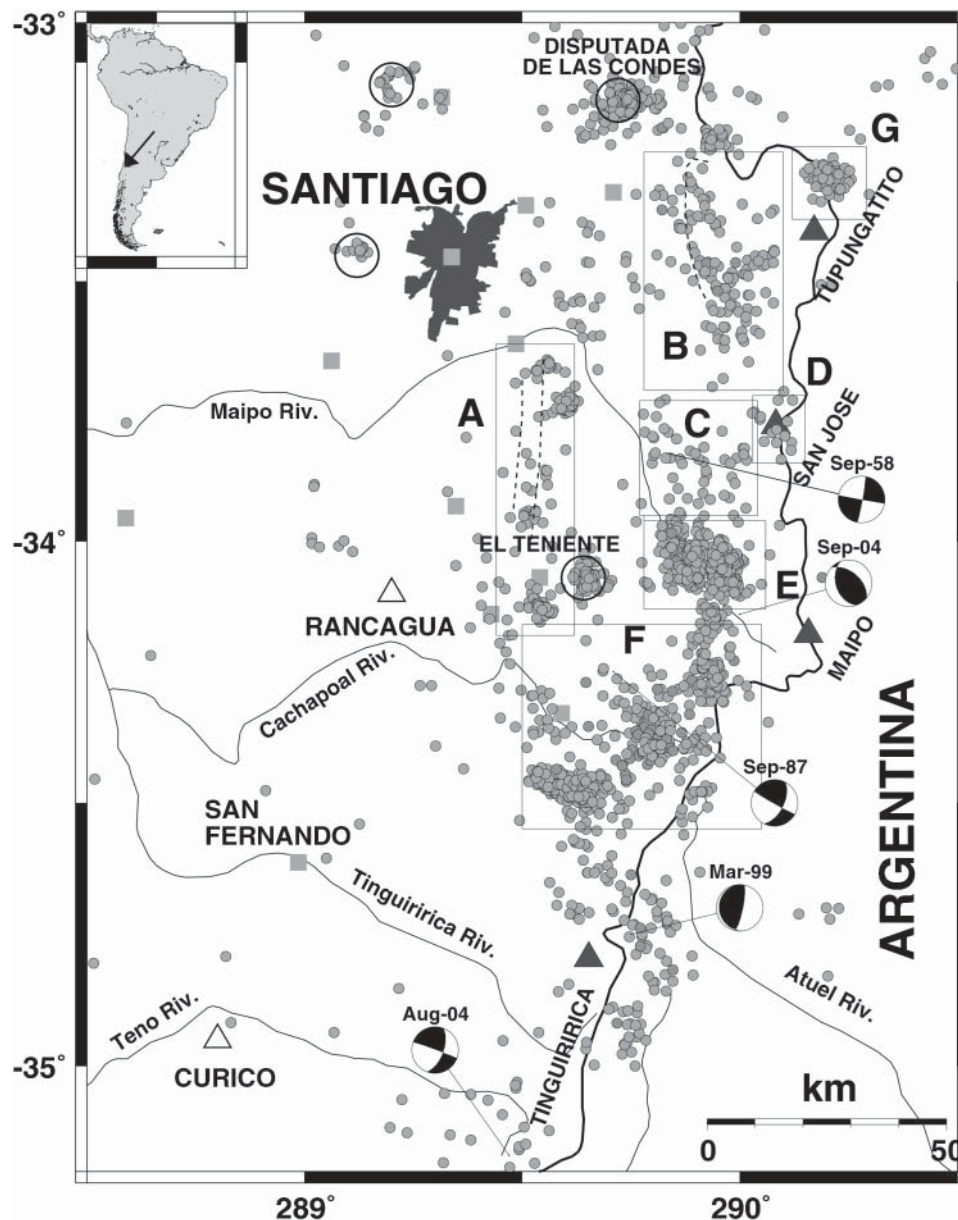


Fig. 10.14. Epicentres of shallow (<20 km depth) earthquakes in the central Chilean Andes during the period 1986–2001 as determined by Central Chile Seismic Network (solid squares). The dashed lines in regions A and B correspond to the lineaments along the Pocomo Fault System (Box A) and Olivares River (Box B) respectively (from Barrientos *et al.* 2004b).

Campos *et al.* 2002). On a few occasions past ruptures from north or south have penetrated into this region. This was the case in 1906 ($M_s = 8.3$) and most likely also during the 1647 and 1730 events, extended from the north and, in 1751, rupturing from the south. The last large magnitude thrust event in this region took place in 1928.

On 20 February 1835 a large earthquake took place in this region. It mainly affected the Concepción area where the damage it produced and the ensuing tsunami were described in detail by Darwin in his book 'Voyage of the Beagle'. At the time of the earthquake, Darwin and Robert Fitz-Roy, the Captain of HMS *Beagle*, were in the area of Valdivia, 350 km south of Concepción. Darwin, who visited the Concepción area 12 days after the earthquake occurrence, included in his reports how the earthquake was felt, the destruction of the city and evidence of uplift of the Concepción Bay and Santa María Island, by nearly 1 m and over 3 m respectively.

Beck *et al.* (1998) analysed in great detail the 1928 Talca and the 1939 events which took place in this region. They concluded

that the 1928 $M_w = 7.9$ event is a shallow underthrusting event with rupture propagating to the south. It generated a 1.5 m local tsunami, therefore much of the deformation must have taken place under the sea bed between the coast and the trench. A 28-s duration of the P-pulse with a rupture velocity of 3 km/s indicates that the 1928 event probably extended for approximately 90 km. From the S-P times for aftershocks recorded in La Paz, Bolivia, it appears that the aftershocks occurred south of the main shock across a north-south area of about 150 km (Kelleher 1972).

The 1939 Chillán event with $M_s = 7.8$, has been the most disastrous earthquake in terms of human life in Chile in historical times: 28 000 deaths and significant damage in the Central Valley between Linares (35.8°S) and Los Angeles (37.5°S), in particular to the city of Chillán (Lomnitz 2004). The consequences of this event were so dramatic that the President of Chile, Pedro Aguirre Cerda, formed a Commission to deal with the catastrophe, to study the cause of such massive destruction. The report of the Commission included a special

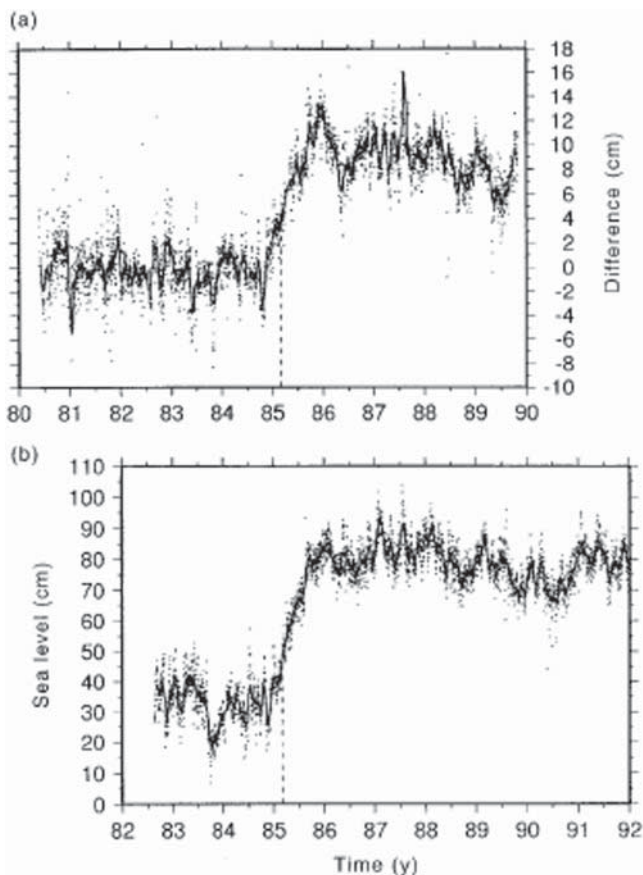


Fig. 10.15. (a) Daily differences of water level at two limnigraphs located at the extremes of Rapel Lake (dots) and its 30-day running average (solid line). (b) Daily values of mean sea-level as a function of time recorded at the Valparaíso tide gauge (dots). The solid line represents a 30-day average. The time of the 3 March 1985 earthquake is denoted by a vertical dashed line in both figures (Barrientos 1997). For references of the locations of Valparaíso and Rapel, see Figure 10.13.

recommendation to establish a building code for the country as a whole. Beck *et al.* (1998) concluded that this event was a product of down-dip tension along the subducting slab at a depth varying between 80 and 100 km (Figs 10.16 & 10.17).

Campos *et al.* (2002) carried out a detailed study of the region between 35°S and 37°S. More than 27 portable stations deployed for three months allowed these authors to estimate the velocity structure, subduction geometry and state of stress. During the period of deployment most of the events took place within the subducting Nazca Plate. Relatively few events were located within the boundary of the two plates. Two other areas of seismicity reported in this study are those at shallow depths near the volcanic zone and in the crust under the Central Valley near the Coastal Cordillera (Fig. 10.18). This latter aspect has not been observed frequently in other regions in Chile, even though local networks have been operating for several decades.

A temporary network of 62 seismological stations, with average 50-km spacing, together with 15 ocean-bottom hydrophones and one bottom hydrophone seismograph, allowed Bohm *et al.* (2002) to locate more than 300 events during three months (January to April 2000). Additionally, six timed chemical explosions were used to produce a refraction profile along 39°S. The Wadati–Benioff zone was observed from 20 km depth to more than 150 km depth (Fig. 10.18) with shallow seismicity restricted to the magmatic arc. A crustal thickness of 40 km was derived from the refraction profile.

Arauco Peninsula–Taitao Peninsula (38–45°S)

The great Chilean earthquake of 22 May 1960, with a surface wave magnitude of 8.5 and a moment magnitude of 9.5, was the largest event recorded in the last century (Kanamori 1977). The quake and subsequent tsunami affected a region inhabited by two and a half million people, and caused over two thousand fatalities (Sievers *et al.* 1963; Plafker & Savage 1970). This event has a special place in seismological history, because it provided experimental confirmation of the idea that earthquakes can cause free oscillations of the Earth (Benioff *et al.* 1961). Nearly all the important cities in south-central Chile from Concepción to Puerto Montt suffered severe damage from shaking which exceeded intensity VIII according to the Modified Mercalli Intensity scale (MMI). Intensities above VIII were registered in areas of poor or unconsolidated soil conditions and sites exposed to topographic amplification. In Chile, for large under-thrusting events beneath the coast, the isoseismal corresponding to intensity VIII roughly mimics the size of the rupture length.

Cifuentes & Silver (1989) determined a magnitude of $M_w = 8.1$ (2×10^{21} N m,) for the foreshock with a rupture length of about 150 km, that took place 33 hours earlier in the northernmost extension of the rupture region (37.03–38.74°S; Plafker & Savage 1970) of the 1960 $M_w = 9.5$ giant earthquake. Cifuentes (1989) suggested that the seismicity shows a southward migrating pattern during these 33 hours. Krawczyk *et al.* (2003) suggested that the hypocentre should be located about 80 km to the west from that reported by Cifuentes (1989), at the interface between the Nazca and South American plates. The total rupture length of the sequence is of the order of 1000 km.

Plafker & Savage (1970) reported coastal elevation changes produced by the 1960 event from Peninsula de Arauco to Peninsula de Taitao, a 1000-km-long segment along the coast of southern Chile. These measurements, carried out in 1968 and based on intertidal algal environment modification and evidence from dead barnacles, balanús and trees, revealed extreme values of 6 m of uplift in Isla Guambín and 2 m of subsidence in the city of Valdivia. Repeated measurements of triangulation as well as levelling were used in their estimation of the earthquake size: a nearly 1000-km-long dislocation with 20 to 40 m of fault displacement. Later, Plafker (1972) reanalysed the static deformation and deduced a causative fault 120 km wide by 1000 km long, dipping 20°E with 20 m of slip. Assuming a rigidity modulus of 5×10^{10} Pa, the total seismic moment reaches 1.2×10^{23} N m or $M_w = 9.3$. Kanamori & Cipar (1974) estimate a moment magnitude of 9.5.

Barrientos & Ward (1990) used the same information collected by Plafker & Savage (1970) to infer a variable slip model of rupture to identify patches of nearly 40 m of displacement in the northern half of the rupture and only 15 m in the southern portion of the rupture (Fig. 10.19) producing a total moment of 1.8×10^{23} N m ($M_w = 9.4$). They proposed that these types of event recur nearly every 400 years, a hypothesis later strengthened by Cisternas *et al.* (2005) from the records of tsunami sands deposited in Maullín, to the west, on the open coast at the latitude of Puerto Montt. Eight occurrences of this type of deposit allowed them to estimate a mean recurrence of the order of 280 years. Curiously, the major event that took place in November 1837 (see Fig. 10.6), which caused a large tsunami across the Pacific Ocean (6 m runup at Hilo, Hawaii; 2 m in Mancera Island, near Valdivia), did not produce a sand deposit in Maullín, so the rupture must have been restricted from Chiloé Island to the south. This is consistent with the lower values of displacement in the southern portion of the 1960 event (Fig. 10.19).

Post-seismic displacements associated with this large event have been reported by Barrientos *et al.* (1992), with observations made in 1991–1992 at several sites previously reported by Plafker & Savage (1970). These observations, together with

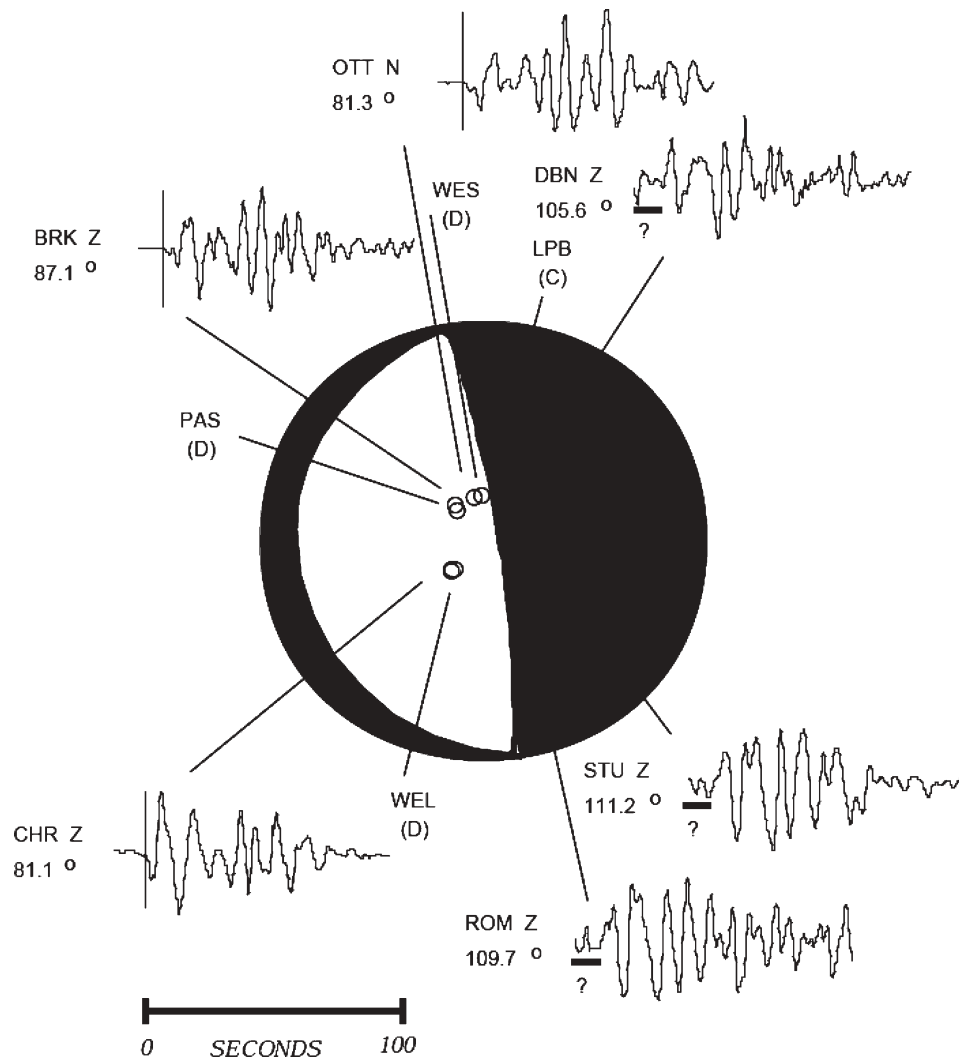


Fig. 10.16. P-wave first motion focal mechanism and waveforms for the 1939 earthquake (Beck *et al.* 1998).

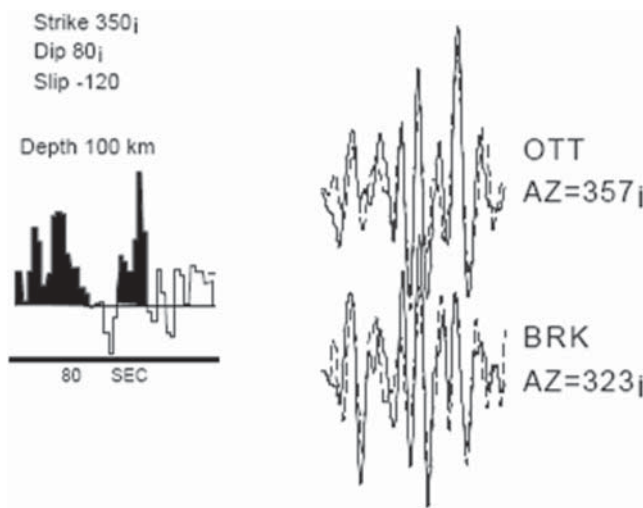


Fig. 10.17. Observed P-waveforms (solid lines) at stations in Ottawa (Canada) and Berkeley (US) and the modelled signals (dashed line) using the focal mechanism shown in the previous figure and source time function on the left. The earthquake depth is 100 km (Beck *et al.* 1998).

measurements at the Puerto Montt tide gauge, indicated continuous uplift of the region. Nelson & Manley (1992) reported on the uplift of Mocha Island before, during and after the 1960 event, with nearly the same amount of elevation change, 1.5 m coseismic and another 1.5 m of post-seismic uplift. Khazaradze *et al.* (2002) interpreted the post-seismic horizontal deformation observed between 1994 and 1996 (Klotz *et al.* 2001) as viscous relaxation of the mantle.

Taitao Peninsula–Puerto Natales (46–52°S)

This is the region in Chile with the lowest rate of seismicity. No field seismic studies have been carried out in the zone except for that of Murdie *et al.* (1993) centred around the Taitao Peninsula. Nine three-component digital seismic stations installed for a period of two months recorded about three local events per day (Fig. 10.20). Nearly 50 well-recorded events allowed Murdie *et al.* (1993) to establish two main observations: (a) a lineament of epicentres interpreted as an active segment of a subducted transform fault, and (b) extensional mechanisms for earthquakes located along the predicted subduction ridge. One of their main conclusions is that extension in the slab influences the overlying crust, giving rise to dextral transtension, and that the pattern of extension is reflected in the development of a basin south of the northward relative subducting ridge.

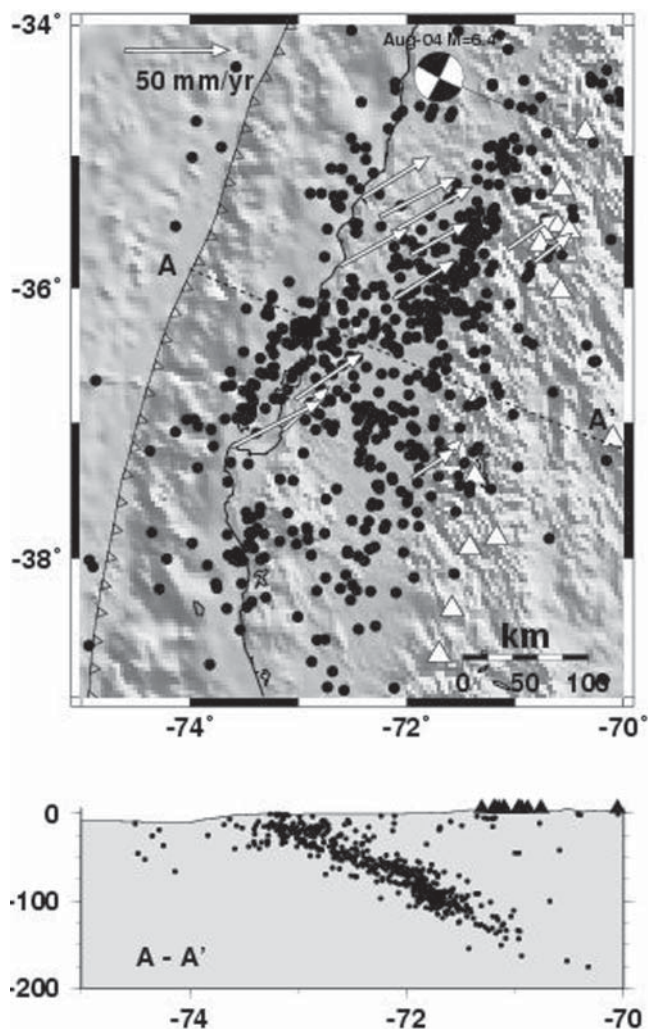


Fig. 10.18. Distribution of well-located earthquakes recorded in three months in the Constitución-Concepción area reported by Campos *et al.* (2002) north of profile A–A', and by Bohm *et al.* (2002) south of profile A–A', and their projection along a profile delineating the Wadati–Benioff zone at these latitudes. Volcanoes are white (top panel) and black (lower panel) triangles. Arrows represent velocities (in mm/year) with respect to stable South America.

Magallanes (53–55°S)

The Magallanes region is generally perceived as fairly aseismic when compared to the rest of the country. Although there might be some truth in this perception, because few shocks are felt during any given year, the seismic hazard is still fairly high. Historical reports indicate that major earthquakes have been felt in Punta Arenas (in 1879 and 1949), probably occurring along the Magellan Fault (Lomnitz 1970; Kleipis 1994). Because Magallanes was a generally uninhabited place in those days, very little is known about the 1879 event, except that it had a significant magnitude, probably greater than 7 (Lomnitz 1970).

The SISRA (catalogue of earthquakes for South America, Centro Regional Para América del Sur, 1985) catalogue lists a magnitude of $7\frac{1}{2}$ for the 1879 event. Two large events that took place on 17 December 1949, the first occurring at 06:53 hours and the second at 15:07 hours, have been listed with magnitudes of $7\frac{3}{4}$ in the SISRA (catalogue). Recent estimations from waveform modelling of teleseismic records of the 1949 events

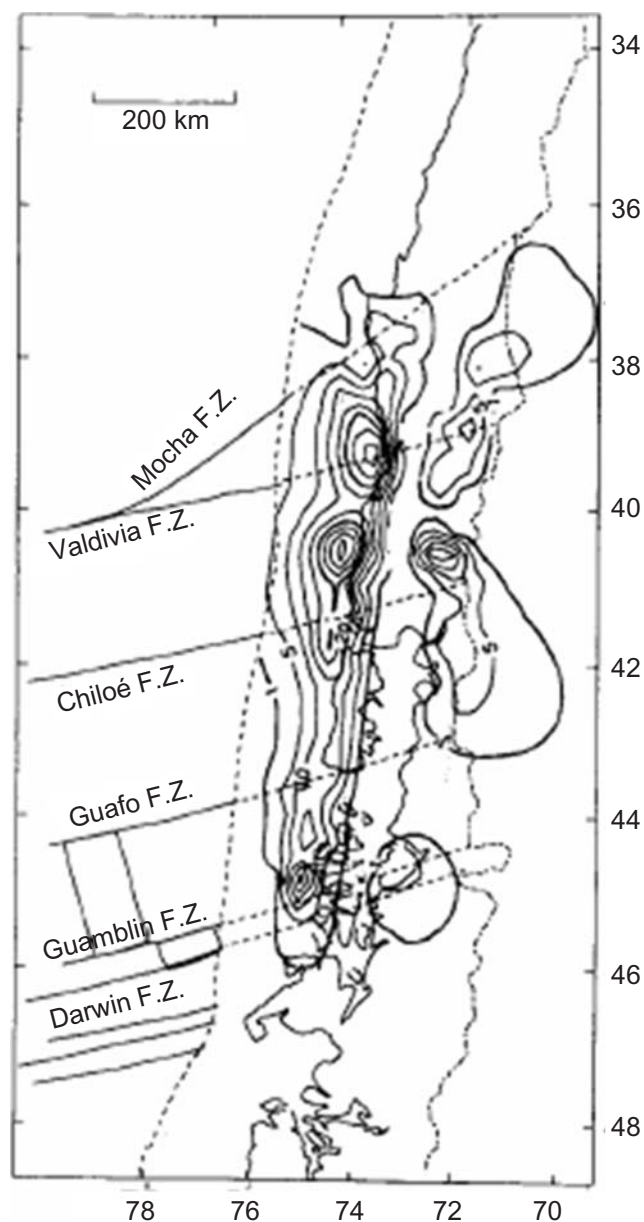


Fig. 10.19. Map of the variable slip distribution and landward extension of the Nazca fracture zones. The 1960 rupture was sharply terminated at the intersection of the Mocha fracture zone in the north and the Taitao Peninsula in the south (46°S). Note that most of the large fault displacement (up to 40 m) is distributed in the northern half of the rupture (after Barrientos & Ward 1990).

also show that the magnitude estimates are in the range of >7 (P. Alvarado, pers. comm.). Figure 10.21 shows the different estimates (Gutenberg & Richter, 1954; International Seismological Summary and Coast and Geodetic Survey) of epicentre locations for the 1949 events. The seismograms (vertical component) at Huancayo (Peru) show that the second event produced somewhat larger surface wave amplitudes. Also, the second event produced higher intensities in Punta Arenas. Smalley *et al.* (2003) report a cut on a road at the eastern end of Lago Fagnano, liquefaction in the floodplain of Rio Grande and 150 km SW of Punta Arenas (Lomnitz 1970) as well as up to 5 m of horizontal offsets of fences in a farm located at the intersection of the Magallanes–Lago Fagnano Fault with the coast. Further examination of GPS data in this region is presented in the next section.

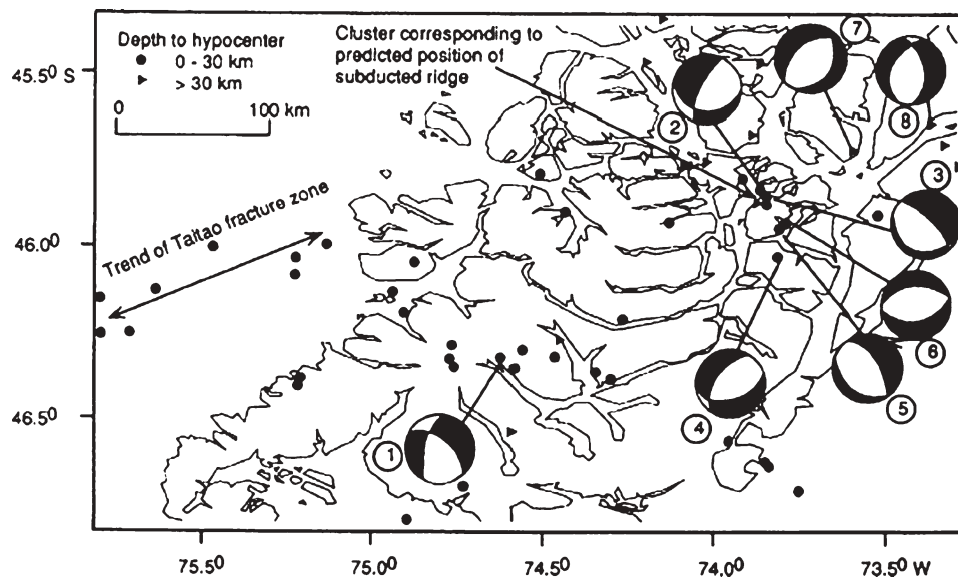


Fig. 10.20. Locations of local earthquakes in the Taitao Peninsula recorded in the first three months of 1992 and their focal mechanisms as reported by Murdie *et al.* (1993). These focal mechanisms probably represent the active extension of the subducted ridge.

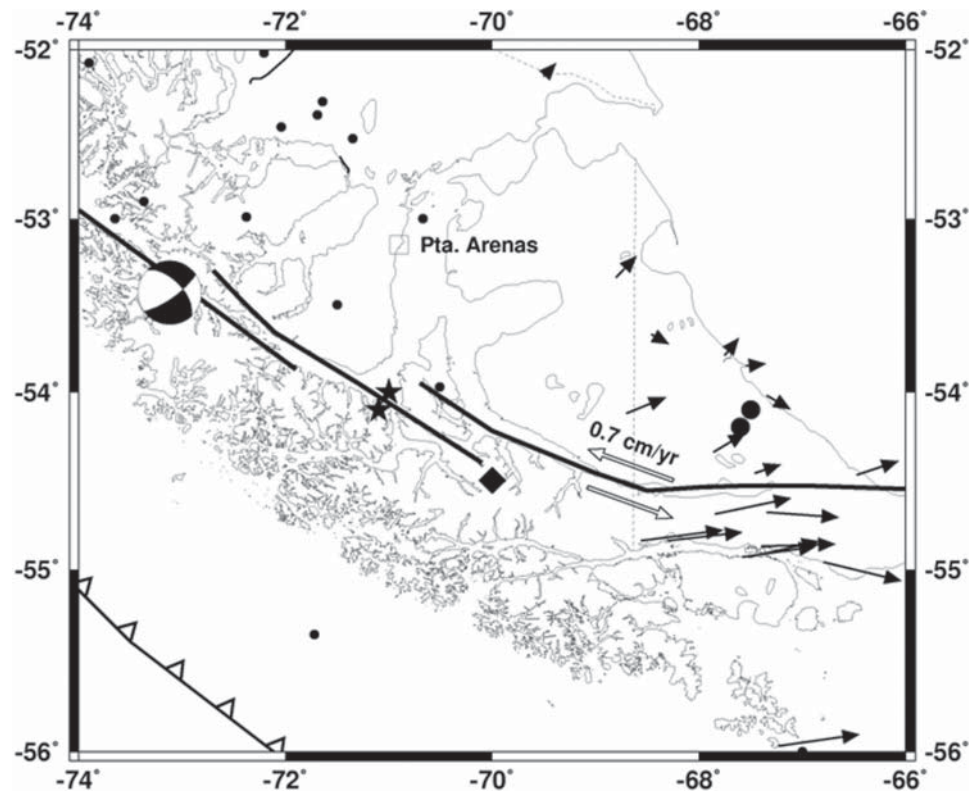


Fig. 10.21. Three segments of the Magallanes–Lago Fagnano Fault which delimits the Scotia and South American plates. The observed velocity on a north–south cross-section is 6.6 mm/year (Smalley *et al.* 2003). The epicentres of the two shocks of 1949 are the solid circles (International Seismological Summary), the two stars (Gutenberg & Richter 1954) and the diamond (US Coast and Geodetic Survey). The only Harvard CMT solution for this region (event on 31 August 1996) is consistent with left-lateral displacement on a fault dipping 59° to the NE.

Adaros *et al.* (1999) reports on a high concentration of earthquakes with focal depths in the range 30–50 km on the western coast of Chile between 52°S and 54°S. They emphasized that few earthquakes took place in Tierra del Fuego itself, but without associating them with any morphological surface structure. This study was based on a five-seismometre deployment for two years in 1997 and 1998.

Summary of the state of stress in the convergent margin (Nazca–South America)

One approach to establish the state of stress in the subduction region is through the observations of deformations, which can be derived from observations using conventional geodetic methods, GPS observations or a combination of both. These

observations are clearly restricted to locations where instruments can be installed, therefore these are land-based methods. A detailed application of the GPS observations in Chile is presented in the next section.

Another approach to examine the state of stress is through indirect observations, such as the type of faulting associated with earthquakes. When an earthquake takes place in a particular region, the waves it generates contain information about the magnitude, energy release, surrounding velocity structure, depth and other information, such as type and orientation of the activated fault. Thus, the information on type of faulting and its conjugate, or earthquake moment tensor, can be extracted from the waves recorded at several different stations worldwide.

The seismology group in Harvard University (<http://www.harvard.edu/projects/CMT>) has carried out routine computations of centroid-moment inversion for earthquakes with magnitude larger than 5.5 worldwide since the mid-1970s. Figures 10.22 to 10.25 show the centroid-moment tensor solutions for the earthquakes in the region of interest (from north to south) during a 26-year period (1980–2005, inclusive). In these four figures, larger symbols represent earthquakes with moment magnitudes (M_w) larger than 6.0 and the dashed line represents the axis of the Peru–Chile trench. Figures 10.22 to 10.24 show moment tensors compatible with low-angle thrust earthquakes distributed along the coast. Further inland, these turn mainly into mechanisms of tensional type, perhaps at depths of the order of about 70–80 km.

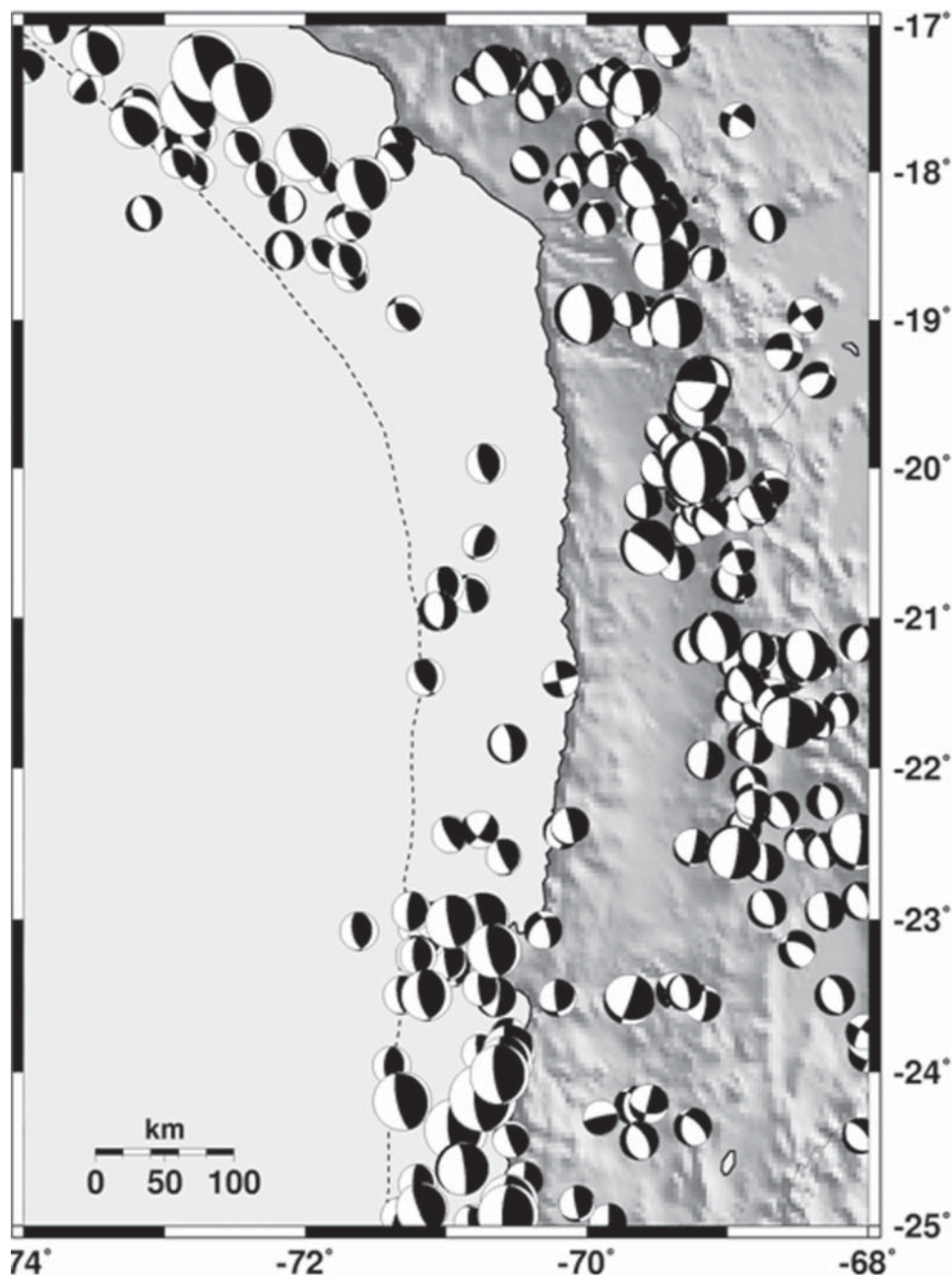


Fig. 10.22. Locations of earthquakes and focal mechanisms listed in the Harvard Moment Tensor site for the period 1980–2005 (inclusive), 17–25°S. The larger circles represent earthquakes with moment magnitudes greater than 6.0. The dashed line corresponds to the location of the Peru–Chile trench. In general, focal mechanisms consistent with low-angle thrust are observed offshore and along the coast; in contrast, focal mechanisms consistent with tensional faulting are observed inland.

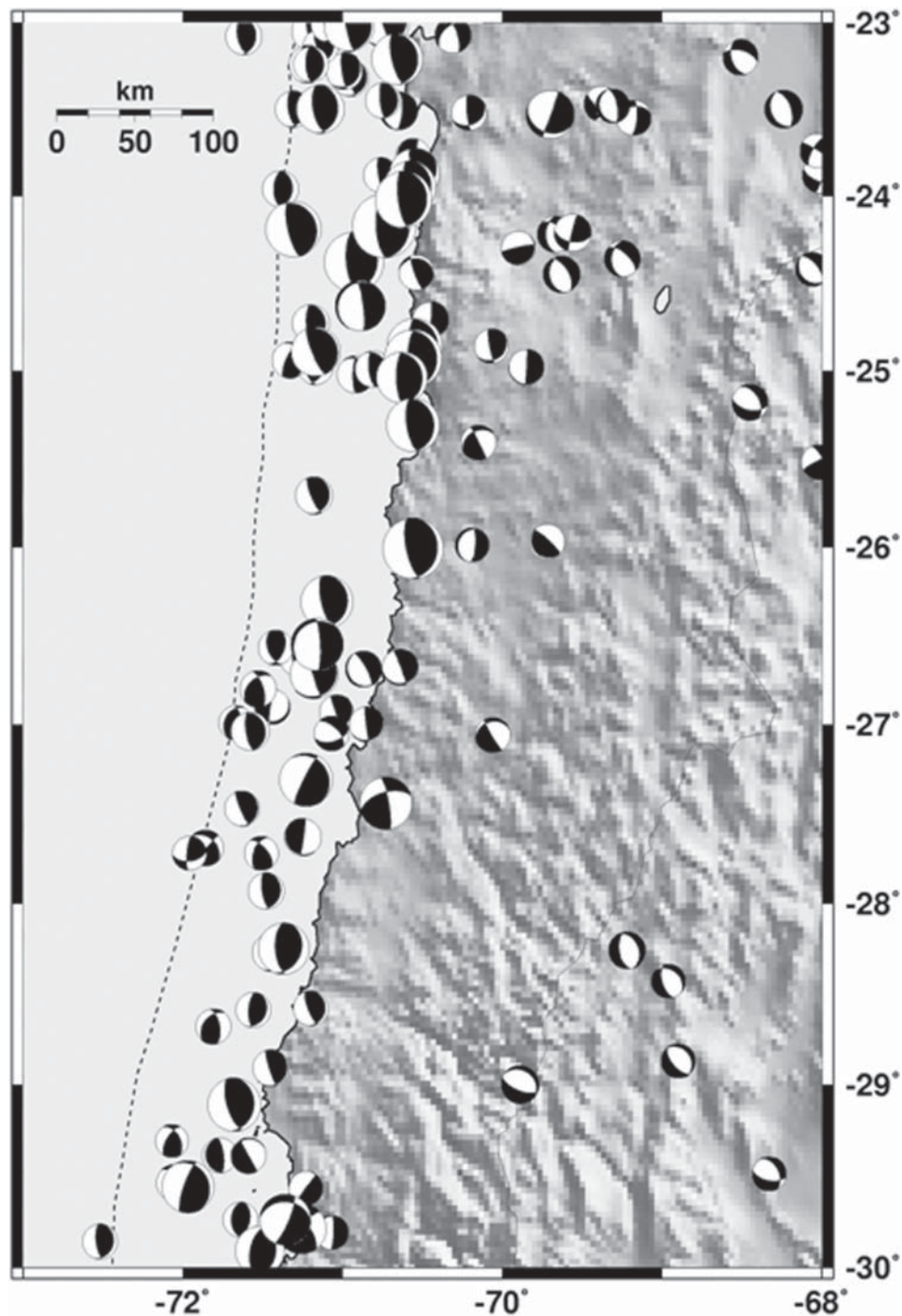


Fig.10.23. Locations of earthquakes and focal mechanisms listed in the Harvard Moment Tensor site for the period 1980–2005 (inclusive), 23–30°S. The larger circles represent earthquakes with moment magnitudes greater than 6.0. The dashed line corresponds to the location of the Peru–Chile trench. In general, focal mechanisms consistent with low-angle thrust are observed offshore and along the coast; in contrast, focal mechanisms consistent with tensional faulting are observed inland.

Figure 10.23 shows thrust-type activity in the region bounded by the coast and the trench. A concentration of activity is evident around 23°S and 24°S, mostly aftershocks of the July 1995 earthquake. The $M > 5.5$ seismicity decreases significantly to the east when compared to the northern region, but the pattern is maintained, mostly tensional faulting.

Major exceptions to the low-angle reverse faulting close to the coast are earthquakes labelled A–D in Figure 10.24. In this figure, B corresponds to the 1997 event described for La

Serena–La Ligua above. Events labelled C and D correspond to normal faults activated as a result of the extension of the upper part of the Nazca Plate due to its initial downward bending. Fromm *et al.* (2006) studied in detail the main event ($M_w = 6.7$) of 9 April 2001 and its 142 localized aftershocks. The seismic clustering in conjugated planes correlates with ridge-parallel fractures observed by bathymetric surveys. Additionally, there are four shallow events (hypocentral depths < 20 km) taking place beneath the Andes south of 34°S, labelled S (Fig. 10.20).

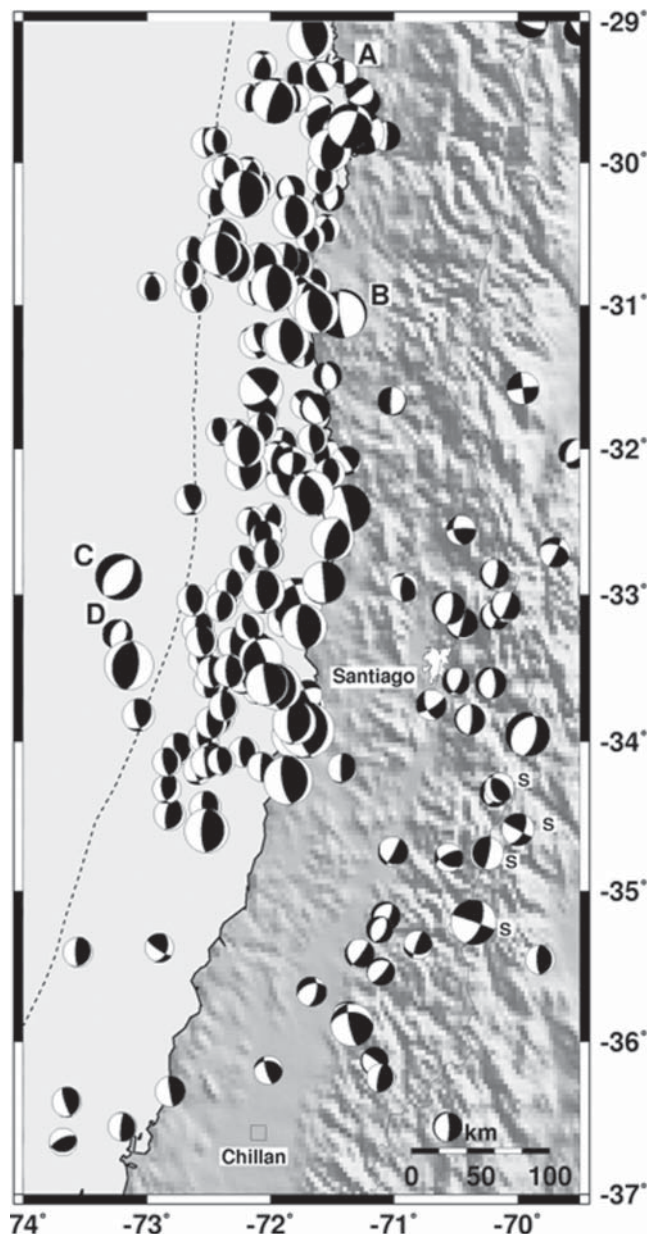


Fig. 10.24. Locations of earthquakes and focal mechanisms listed in the Harvard Moment Tensor site for the period 1980–2005 (inclusive), 29–39°S. Focal mechanisms of earthquakes labelled A and B (the latter corresponds to the October 1997 event) represent faulting on a vertical plane within the subducting Nazca Plate with the trench-ward block down-dropping with respect to the eastern block. Events C and D represent tensional faulting within the Nazca Plate. Four events taking place in the Andes south of latitude 34°S marked with S correspond to shallow events (hypocentral depth < 20 km).

Two of these events show a strike-slip mechanism (right-lateral slip, assuming a north-south fault plane). The northernmost event evidences a NE–SW compression, similar to the strike-slip events, resulting in a roughly 45° angle fault plane dipping to the NE or the SW. The mechanism of the fourth event represents a vertical fault.

Figure 10.25 shows an anomalous pattern when compared to the previous three figures. All moment tensors located offshore south of 39°S indicate an extensional regime. This means that the Nazca Plate is still being pulled, most likely due to post-seismic adjustment after the giant 1960 earthquake. The rectangle and star at 38°S represent the 1960 epicentral

locations proposed by Cifuentes (1989) and Krawczyk *et al.* (2003), where rupture began its propagation southward, eventually reaching the Taitao Peninsula, close to 46°S. Two other interesting features can be observed in this figure: (a) the mechanism of the event south of the city of Chillán, and (b) the shallow earthquakes with strike-slip mechanisms labelled S. As mentioned earlier, the 1939 Chillán earthquake was particularly catastrophic. The fault mechanism proposed by Beck *et al.* (1998) for the 1939 event is consistent with the type of faulting derived for the earthquake located just south of Chillán, which took place in September 1986 at around 80 km depth. Two shallow ($h < 20$ km) events of interest are those labelled S: if the north–south plane is the rupture plane, it means that these events represent right-lateral displacement which would be consistent with the expected displacement along the Liquiñe–Ofqui Fault (described in other chapters and in Cembrano *et al.* 1996).

Comte & Suárez (1994) used complementary information of the state of stress in the convergent zones at depth of about 100 km, from the analysis of data recorded in two microseismic experiments in northern Chile, at the latitudes of the cities of Iquique and Antofagasta (see Fig. 10.5) and at depths of about 100 km. They found evidence of a double seismic zone in which down-dip tensional events were consistently shallower than a family of compressional earthquakes. They interpreted the extensional regime as a result of basalt to eclogite transformation in the subducted oceanic crust, which also produces compression in the underlying mantle. Local studies such as this (Comte & Suárez 1994) can only be carried out with local, denser seismic networks.

Global Positioning System efforts

The rapid convergence rate between the Nazca and South American plates makes this region an excellent laboratory to test ideas about the seismic cycle. In fact, the 1995 Antofagasta earthquake took place in an area where previous GPS observation had been made. Both Ruegg *et al.* (1996) and Klotz *et al.* (1999) reported a maximum horizontal displacement of the order of 80 cm to the west at the coast near Antofagasta. Current estimations of the displacement field at the coast are of the order of 20–30 mm/year in the opposite direction, revealing the deformation to which the region is subjected during the interseismic period of stress accumulation.

Three large continuing efforts can be identified (Fig. 10.26): (a) South America Geodynamics Activities (SAGA) (Klotz *et al.* 2001; Khazaradze & Klotz 2002); (b) Central Andes GPS Project (CAP) (Bevis *et al.* 1999, 2001, 2004; Kendrick *et al.* 1999; Smalley *et al.* 2003); and (c) local efforts (Ruegg *et al.* 1996, 2002; Chlieh *et al.* 2004). All these works present results of GPS observations in Chile, with SAGA and CAP at a global level and the more localized efforts of Ruegg in northern Chile and around the area of Constitución–Concepción. Results of repeated observations in different epochs have been shown already in Figures 10.7 and 10.18. Figures 10.22 and 10.23 show the observation points and results of the SAGA effort.

The velocity field of the coastal region between 26°S and 37°S is characterized by convergence roughly parallel to the relative convergence direction of the Nazca and South America plates at a rate of 3.5 cm/year (Klotz *et al.* 2001) (Fig. 10.27). This rate decreases with distance from the coast. The authors interpret these observations as velocities produced by the interseismic strain accumulation due to 100% locking of the interface between the Nazca and South America plates. To the north of 26°S and to the south of 37°S the regions are dominated by post-seismic effects of the 1995 and 1960 events.

Bevis *et al.* (2001) invoked both elastic loading (as was done in the previous case, by locking of the boundary between the Nazca and South America plates) and backarc convergence

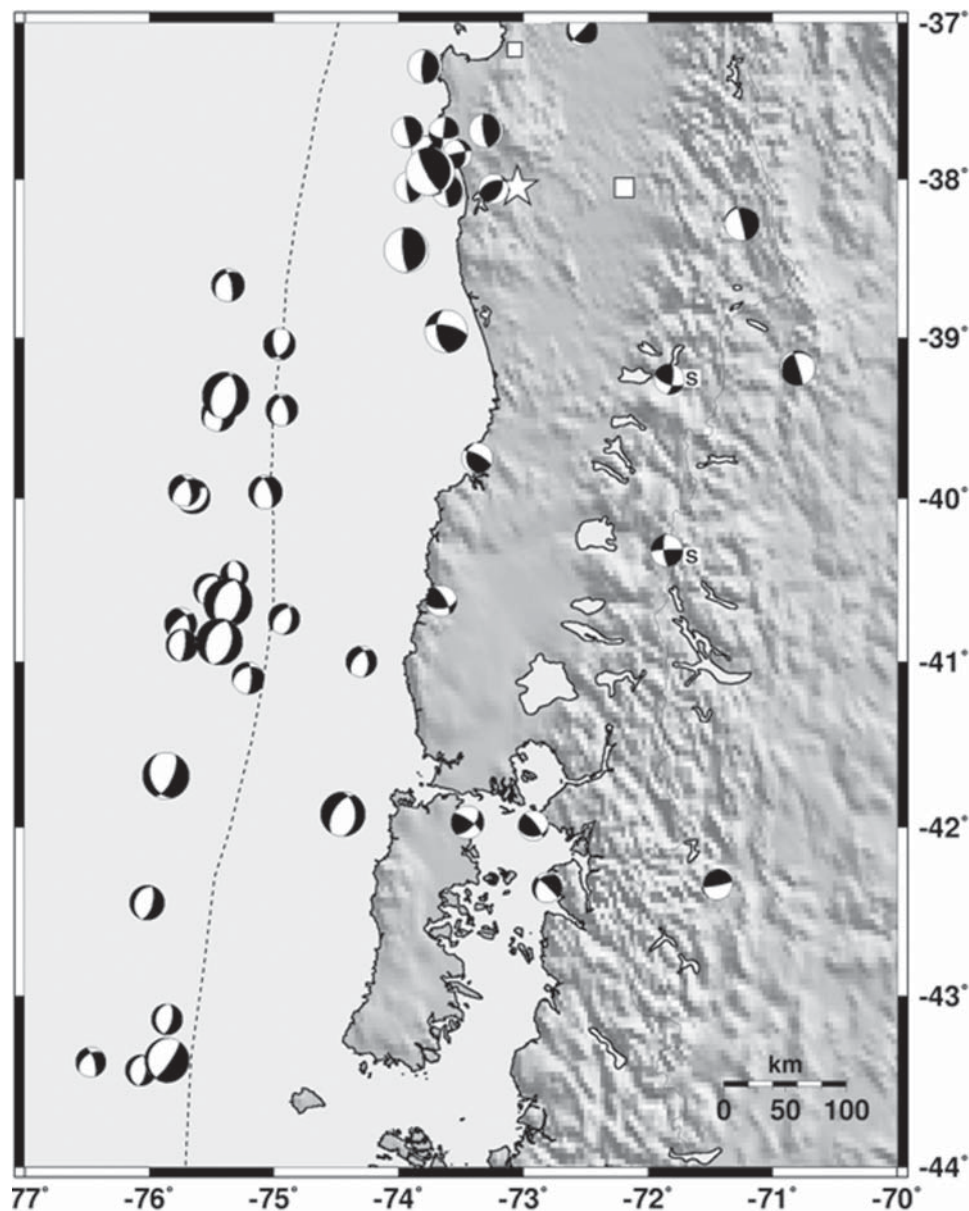


Fig. 10.25. Locations of earthquakes and focal mechanisms listed in the Harvard Moment Tensor site for the period 1980–2005 (inclusive), 37–44°S. Most of the seismic activity is concentrated offshore the trench south of 38.5°S. Focal mechanisms reflect an extensional regime up-dip of the region involved in the 1960 rupture. The large white square represents the epicentral location of the main events of the 1960 sequence (Cifuentes 1989), the small square represents the epicentre of its main precursor, one day before, and the large star is the proposed epicentral location of the main event according to Krawczyk *et al.* (2003).

(5–6 mm/year, or 8.5% of the total Nazca–South America convergence rate) to explain the deformation (velocity field) of the southern Peru–northern Chile region. They concluded that in this region there is no evidence of slip partition.

Additionally, Figure 10.21 shows the estimated displacement in the area close to the Magallanes–Lago Fagnano Fault zone (Pelayo & Wiens 1989) and the measurements after repeated GPS observations in 1998, 1999 and 2000 (Smalley *et al.* 2003). Repeated GPS observations indicate that the deformation zone is not restricted to a linear feature but, as expected in strike-slip regimes, the stress accumulation is dependent on the locking depth of the brittle region. Smalley *et al.* (2003) modelled this velocity field as a vertical fault with 15 km locking depth and a velocity of 6.6 mm/year. From reports of 5 m offsets during the 1949 event, Smalley *et al.* (2003) suggest a return period of the order of 750 years for this segment of the fault. In addition,

GPS reveals that the whole southern Patagonia region is moving to the east in relation to stable South America at a rate of approximately 1.5 mm/year.

Brooks *et al.* (2003) proposed an interesting model to explain the deformation field across the Andes between 26°S and 36°S with respect to the craton. By selecting this region, they avoided possible contamination of the data with the post-seismic effects of the 1995 earthquake in northern Chile and the post-seismic effects of the 1960 southern Chile event. Measurements carried out between 1993 and 2001 reveal that Andean locations show eastward velocities ranging from approximately 35 mm/year close to the Nazca boundary to basically zero (within the error ellipses) in the craton. No oblique deformation is obvious from these measurements. Their results suggest that the oceanic Nazca Plate is fully locked while the continental backarc boundary creeps continuously at around 4.5 mm/year.

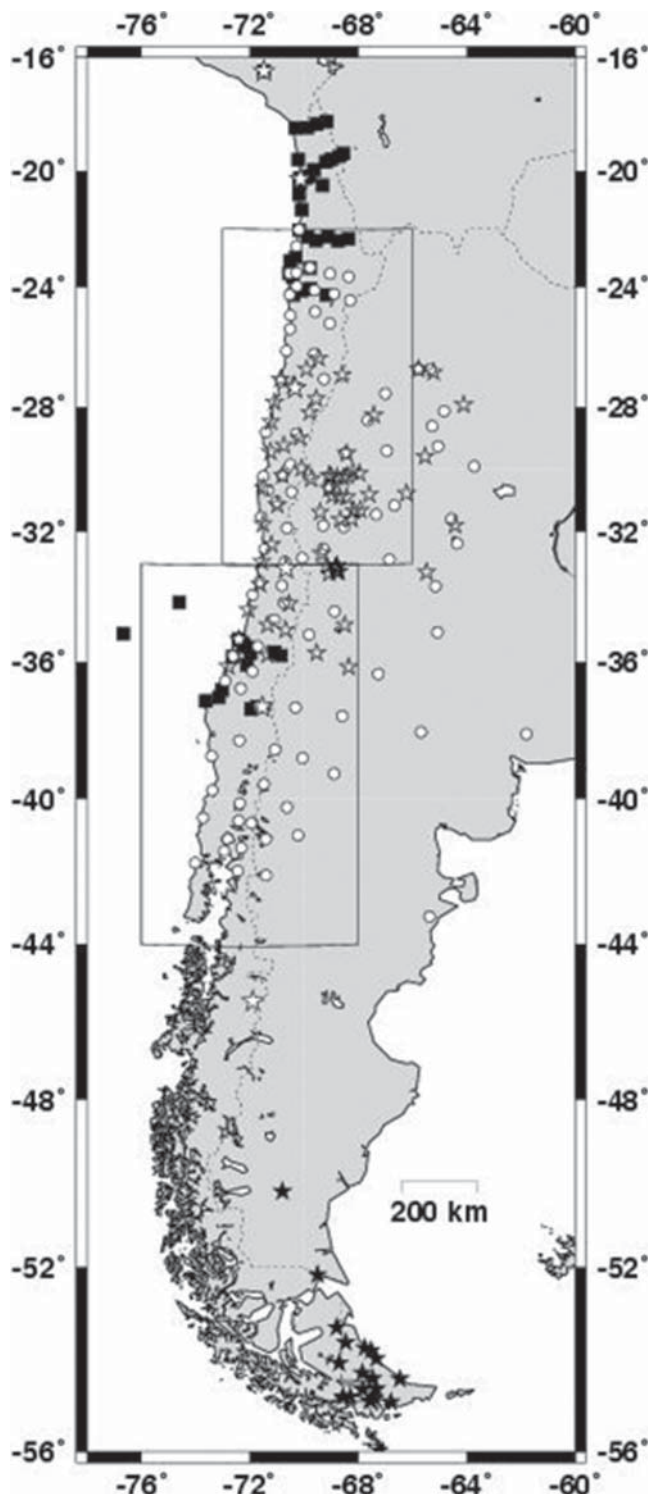


Fig. 10.26. Locations of GPS observation points of three different efforts: SAGA (circles, Klotz *et al.* 2001); CAP (open and solid stars; Bevis *et al.* 2001; Brooks *et al.* 2003; Smalley *et al.* 2003) and local efforts of Ruegg and collaborators (solid squares; Ruegg *et al.* 1996, 2002). The two rectangles show points of estimated velocity field in Figure 10.23.

Seismic hazard assessment in Chile

Seismic hazard is, by definition, one of the two major components of seismic risk assessment, the other being vulnerability. The product of seismic hazard and vulnerability

of structures provides the basis on which key planning and evaluation studies can assess the different risk levels for existing and future buildings and works of infrastructure at any given site. The main goal of seismic hazard assessment is to estimate, within a period of interest, the characteristics of the expected ground motion, which can be expressed in terms of intensity, ground displacement, velocity or acceleration. The possible consequences of this movement on the ground itself (e.g. liquefaction) and the soil response are also part of the earthquake hazard estimation.

In principle, a long history of records at any site should provide enough information to estimate future ground motion. Unfortunately, this is not possible everywhere because not all sites have been adequately covered by appropriate instrumentation, and the long history of records is not long enough compared with the return periods of large earthquakes, which are the most dominant in the estimation of hazard. In the case of Chile, these large events, with magnitudes of the order of 8, involve the whole width of the coupling region within the subduction zone and have return periods of about 100 to 150 years (Lomnitz 2004). Furthermore, it has been postulated that magnitude 9+ earthquakes might have recurrence periods of the order of 300 years or more (Cisternas 2005; Barrientos & Ward 1989). Lomnitz (2004) states that even at these long scales, the moment release is not constant. In the case of central Chile he proposes that there has been an acceleration of moment release after the large 1822 earthquake.

First estimations of seismic hazard were carried out by Lomnitz (1969) who, using a probabilistic method, only considered events larger than 7½ because smaller ones do not significantly contribute to the seismic hazard and therefore can be disregarded. According to Lomnitz (1969) these medium to large-magnitude events produced a Modified Mercalli Intensity (MMI) over VI. To enable probabilistic estimations, he assumed that the seismic sources follow a Poisson distribution and the isoseismal VI represents a level of 0.1g in acceleration.

This idea is expressed as R_i in the equation

$$R_i = 1 - e^{-\frac{n_i t}{T}}$$

in which R_i is the seismic hazard (Lomnitz used the term 'risk'), T is the length of the whole earthquake record, n_i is the number of events that produce an MMI of VI or greater during T , and t is the design period

Explicit attenuation relationships were not used in this approach, although they were included in the determination of the isoseismal VI (MMI), with the maximum extent of the hazard depending on the attenuation of the intensity with distance. Lomnitz (1969) published estimated probabilities with an exceedance of 0.1g over a period of 30 years, emphasizing the fact that what is important is the number of times this level (0.1g) is exceeded, not by how much.

More recently Barrientos (1980) and Martin (1991) have developed probabilistic estimations of the seismic hazard for the country as a whole. Based on the method proposed by Algermissen & Perkins (1976), both studies include a characterization of the seismicity based on: (a) determination of the seismogenetic sources, (b) earthquake 'productivity', defined as the number and relative size of the events in terms of the distribution ($\log N = a - b M$), and (c) the expected maximum magnitude that earthquakes can reach within each region. According to Algermissen & Perkins (1976), in a no-memory Poisson model, estimation of the return periods of an event exceeding a given level of acceleration (or ground motion) is the reciprocal of its annual probability of exceedance. In calculations of seismic hazard, as Lomnitz had proposed in 1969, the desire is to estimate the probability of exceeding the level of ground motion within a certain period T (e.g. the lifetime of a

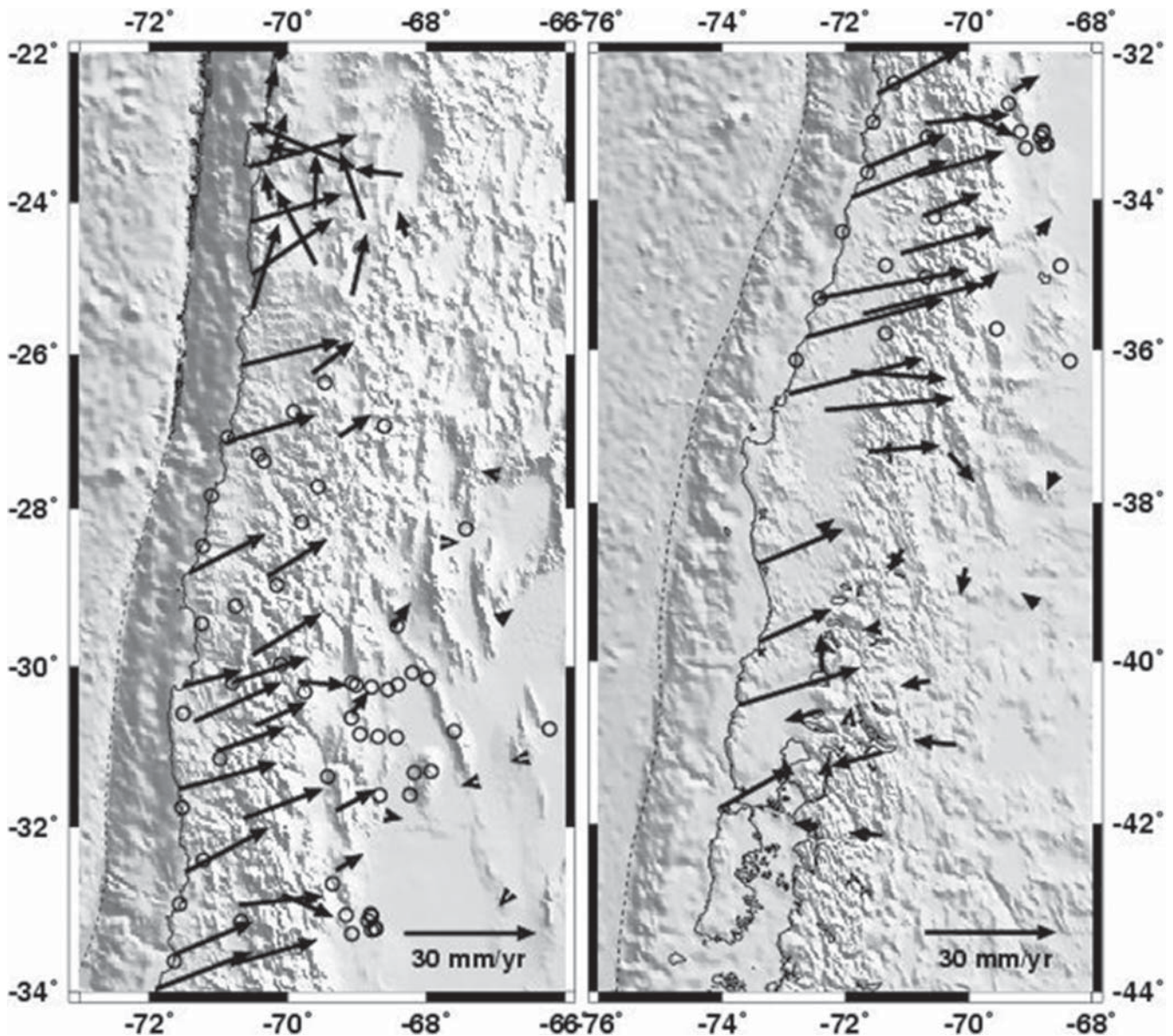


Fig. 10.27. Horizontal velocity field (in mm/year), derived from several campaigns during the 1990s (Klotz *et al.* 2001). Measurements between 23°S and 24°S were carried out after the July 1995 Antofagasta earthquake. The main feature of this field is characterized by velocities of 20 to 30 mm/year along the coast orientated in an ENE direction. The region south of 37°S still shows the effects of the giant 1960 earthquake.

structure), then the return period is related to that probability according to: $P(t) = 1 - t/T$.

Barrientos (1980) divided the seismogenic zone in eight different regions (four coastal and four cordilleran) with different values of a and b , the coefficients of the frequency-magnitude distribution. In his study, the subdivision of coastal and cordilleran regions was based on those events located shallower or deeper than 50 km, respectively, recognizing the down-dip limit of the rupture zones of large subduction events. An attenuation relationship on Modified Mercalli Intensity of the type

$$I(r) = 1.38M_s - 3.74 \log(r) - 0.0006r + 3.91$$

where M_s is the event magnitude based on surface waves and r is the epicentral distance or the distance from the site of interest to the closest point of the fault (Fig. 10.28), allowed Barrientos (1980) to estimate intensities with a 10% probability of being exceeded in 50 years.

Martin (1991) estimated accelerations not to be exceeded within a period of interest (50 and 100 years). For this, he collected all maximum vertical and horizontal accelerations recorded on rock due to earthquakes in Chile and summarized them in an attenuation relationship of acceleration as a function of magnitude and distance of the type:

$$a = \frac{71.3}{(R + 60)^{1.03}} e^{0.83M_s}$$

The expected peak accelerations as a function of distance (R) for different magnitude events taking place at a depth of 30 km are shown in Figure 10.29. Peak accelerations nearly half that of gravity are expected in the neighbourhood of the surface projection of the fault for a large-magnitude event, while a magnitude 5 tremor would not generate more than 5% of g . Figure 10.30 shows the peak accelerations with a 10% chance of being exceeded during a 50-year term. As expected, higher peak

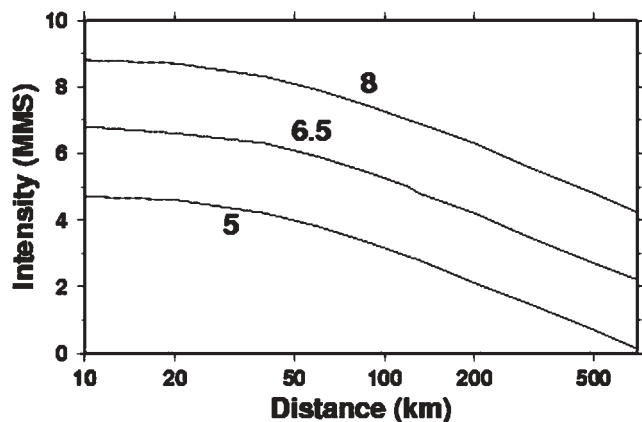


Fig. 10.28. Intensity attenuation as a function of distance for different magnitudes according to Barrientos (1980).

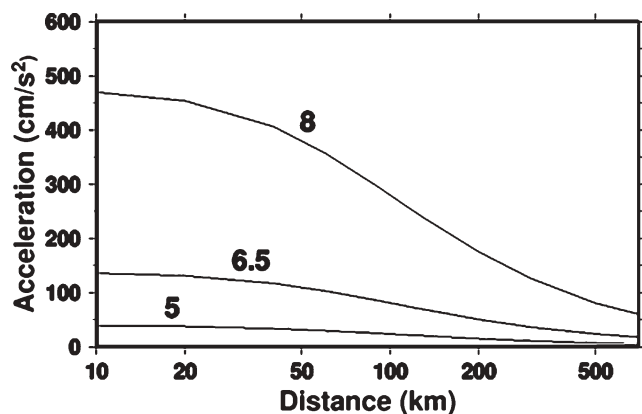


Fig. 10.29. Horizontal acceleration attenuation as a function of distance for different magnitudes according to Martin (1991).

accelerations are located closer to the coast due to the location and depth of the large thrust events that dominate the seismicity in the region. Two zones are of additional interest in this map, both dominated by shallow (less than 20 km depth) seismicity. One of these is in response to plate shortening (in the Andes, between 30°S and 35°S latitude, and continuings to be well developed into Argentina; Alvarado *et al.* 2005), whereas the other is attributed to transcurrent displacement (Magallanes region) which give rise to earthquakes such as those occurring in 1949 (Klepeis 1994).

In these approaches, there has been no attempt to include aspects related to local effects, which depend on the geometric and physical conditions of the site. Localized studies have been attempted in various cities in Chile but no uniform and standardized approach has yet been proposed. Additional elements of seismic hazard which will eventually be included in estimations are, among others, rupture directivity and variations of stress-drop associated with inter- and intraplate events, examples of the effects of which are beginning to emerge.

Discussion

The dominant aspect of seismicity in Chile is controlled by the subduction of the Nazca Plate under the South America

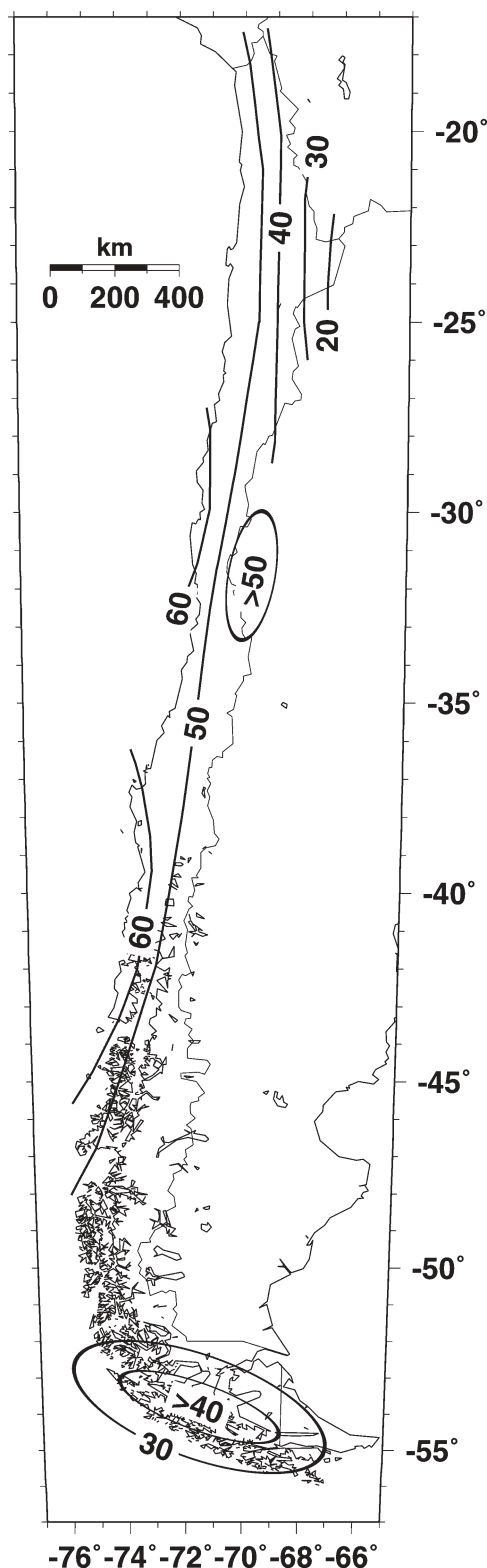


Fig. 10.30. Peak accelerations with a 10% chance of being exceeded during a 50-year term (Martin 1991). Higher peak accelerations are expected closer to the coast due to the location and depth of the large thrust events that dominate the seismicity in the region. Two zones are of additional interest in this map, both dominated by shallow (less than 20 km depth) seismicity: the Cordilleran region between 30°S and 33°S and the southern extreme, in Tierra del Fuego (53°–55°S). The next generation of this type of map should include the effects of higher stress-drop events (7–100 km depth) tensional faulting and the recognized southward extension (at least to 35°S) of the shallow cordilleran region.

Plate. This subduction, however, is not regular throughout the convergence margin. The age of the subducting Nazca Plate varies from 90 Ma at 17°S to 0 at the triple-junction near 46°S. Furthermore the region between 26°S and 33°S is characterized by the gradual southward decrease of the dip angle of subduction, the absence of a central valley between the Coastal Cordillera and the Andes, and lack of recent volcanism due to the buoyancy of the subducting Juan Fernández Ridge (Gutscher *et al.* 2000b).

It is clear that, with the possible exceptions of Mejillones and Arauco peninsulas (and certainly the Taitao Peninsula), there is no particular segmentation of the rest of the coupled region along the coast of Chile. The 1000-km-long 1960 rupture had been previously partially ruptured by the 1737 and 1837 events, with only the 1575 earthquake being of a similar size. Analysis of tsunami deposits indicates that 1960-type events recur in the region about every 300 years. The central Chile region is another example of variability of consecutive ruptures; the largest event in the sequence of historic earthquakes, which begins in the mid-1500s with the Spanish conquest, is the 1730 event which had a source length of more than 500 km. One interesting observation is that all the underthrusting earthquakes studied in any detail have shown that their rupture begins in their northern part, and their ruptures propagate to the south.

Not only do the large magnitude earthquakes differ in size from cycle to cycle but also in the manner in which the convergence between the two plates is accommodated. The July 1995 Antofagasta earthquake showed only a small post-seismic readjustment towards the north of the coseismic rupture, under the Mejillones Peninsula. In contrast, continuous records of tilt and tide gauges at the coast above the rupture region in Vaparaíso revealed that an eight- to ten-month process was dominant in accommodating the deformation. Another is the case of the 1000-km-long rupture produced by the 1960 megathrust event, with post-seismic readjustments still being measured by GPS techniques 45 years after its occurrence.

Another interesting aspect of seismicity in Chile is the increasing evidence for shallow seismicity in the Andes and/or its foothills throughout the whole country. Even though no surface evidence of rupture was found for the September 1958 Las Melosas (Upper Maipo Valley, SE of Santiago) earthquake ($M=6.9$), it was clearly documented as a shallow event, Lomnitz (1961) assigned a local intensity of X (MMI). A recent example of a shallow event ($M=6.4$) in August 2004 reminds us of the southern extension of these seismic sources and the need for a reconsideration of their importance to seismic hazard evaluations. Another relatively large shallow event ($M=6.3$) took place in July 2001 on the western flank of the Andes in northern Chile. Temporary networks have demonstrated the existence of shallow crustal seismicity in varying degrees along the country.

In summary (Fig. 10.31), the potential areas most subject to large-magnitude earthquakes lie above the coupling region

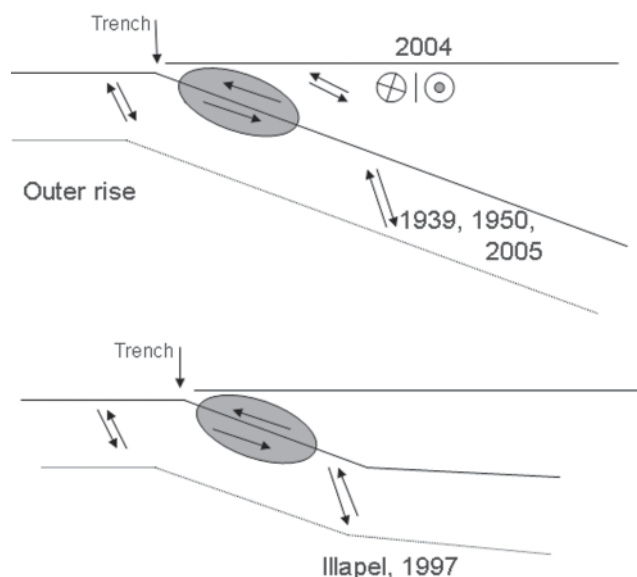


Fig. 10.31. Summary of different modes of fault mechanisms in the Nazca–South America plate subduction region in Chile. Off-trench compressive and tensional fields are present. Strike-slip faulting is also present along the Liquiñe–Ofqui Fault as well as in the Magallanes Fault zone.

between the Nazca and South American plates, which corresponds to the contact region between the trench and approximately 45–53 km depth along the Wadati–Benioff region. Earthquakes in intraplate regions within the subducting Nazca Plate, which can reach magnitudes of the order of 8, are characterized by higher stress drops than events that take place in the contact between these two plates, thus producing higher accelerations at the surface. Large magnitude earthquakes are also generated at the transcurrent system between the South America and the Scotia plates. We have come a long way from the early reports of Maria Graham and Charles Darwin, and the overall controls on Chilean seismicity are clearly much better understood. Whilst future studies will continue to improve our knowledge of the seismic pattern, much work also needs to be done on prediction and damage limitation in this spectacularly earthquake-prone country.

I would like to thank S. Beck, C. Lomnitz, T. Monfret and J. Klotz for providing many important suggestions that made this article more accurate and readable. Most of the figures were prepared using the Generic Mapping Tools (GMT) software (Wessel & Smith 1991). I would like to thank the support of the Millennium Initiative on Seismotectonics and Seismic Hazards.